Corp., MA, USA) with the oligonucleotides containing the multi-cloning sites. The *SalI/EcoRI* fragment of pHM15-A35-1 (bp 23583-27760) was inserted between the *SalI/EcoRI* sites of pFS1-Ad35-1, resulting in pFS1-Ad35-2. pFS1-Ad35-2 was then cut by *EcoRI/BamHI* and ligated with oligonuclotide 4 (5′-AATTGGCCACG TAGGCC-3′) and 5 (5′-GATCGGCCTACGTGGCC-3′) (*SfiI* recognition sequence is underlined), resulting in pFS1-Ad35-9. The *SalI/NotI* fragment of pFS1-Ad35-9 was ligated with the *SalI/NotI* fragment of pHM14-Ad35-1, creating pHM14-Ad35-3. pHM14-Ad35-1 was constructed by cloning of the *EcoRI/KpnI* fragment (bp 21945–29545) of the Ad35 genome into the *EcoRI/KpnI* sites of pHM14.[53] The *EcoRI/NotI* fragment of pHM14-Ad35-3 was ligated with the *EcoRI/NotI* fragment of pAdMS1, resulting in pAdMS3-1. The *NotI* site of pAdMS3-1 was changed into an *SbfI* site by using oligonucleotide 3, resulting in pAdMS3. The *SbfI/AscI* fragment of pFS2-Ad35-11 was ligated with the *SbfI/AscI* fragment of pAdMS3-1, creating pAdMS4-1. The *NotI* site of pAdMS4-1 was changed into a *SbfI* site by using oligonucleotide 3, resulting in pAdMS4. pAdMS2 and -4 have I-*CeuI*, *SwaI*, and PI-*SceI* sites in the E1 deletion region (ΔE1: bp 368–3374). pAdMS3 and -4 have an *SfiI* site in the E3 deletion region (ΔE3: bp 27 761–29 731). The E1a and E1b coding regions of Ad35 are located from bp 569 to 1441 and from bp 1611 to 3400, respectively, according to the Ad35 genome sequence (GenBank Accession No. AY271307). The E3a and E3b coding regions of Ad35 are located from bp 27 199 to 29 496 and from bp 29 538 to 30 622, respectively. pAdMS2, -3, and -4 have *SbfI* sites at both ends of the Ad genome.

Shuttle plasmids containing a variety of promoters were constructed by changing the CMV promoter of pHMCMV5[21] into another type of promoter, including the EF1α promoter, the CA promoter, the mouse PGK promoter, the MSCV promoter, and the CMVi promoter. The EF1α promoter is derived from pEF1α/myc/nuc (Invitrogen, Carlsbad, CA, USA). The CMVi promoter is derived from pGeneGrip (Gene Therapy Systems, San Diego, CA, USA). The composite CA promoter and PGK promoter were kindly provided by Dr J Miyazaki (Osaka University, Osaka, Japan) and Dr MA Kay (Standford University, CA, USA), respectively. The MSCV promoter was a kind gift of Dr RG Hawley (American Red Cross, MD, USA).

E1/E3-deleted Ad35 vectors expressing enhanced GFP

To construct the plasmid for a recombinant E1/E3-deleted Ad35 vector containing a CMV promoter-driven GFP expression cassette, pHMCMV-GFP1[54] and pAdMS4 were digested with I-*CeuI* and PI-*SceI*. The digested pAdMS4 was ligated with the I-*CeuI*/PI-*SceI* fragment of pHMCMV-GFP1 containing a GFP expression cassette, resulting in pAdMS4-CMVGFP. pAdMS4-CMVGFP was linearized by the digestion with *SbfI*. The linearized DNA was transfected into VK10-9 cells (kindly provided by Dr V Krougliak),[22] which are 293 cells expressing the E4 proteins of Ad5 as well as the E1 proteins. A cytopathic effect (CPE) was observed 10–14 days after transfection, and the virus was then amplified in VK10-9 cells and purified by the conventional method for Ad5 vector preparation. For the preparation of recombinant E1/E3-deleted Ad35 vectors containing various types of promoters, a *GFP* gene was cloned into multi-cloning sites in the shuttle plasmids containing various types of promoters, and the Ad35 vectors were then prepared by methods similar to those described above.

Transduction experiment

Human bone marrow CD34$^+$ cells were purchased from Biowhittaker, Inc., Walkersville, MD, USA. The cells were recovered from the frozen stock, suspended in StemSpan™ 2000 containing cytokine cocktail StemSpan™ CC100 (human Flt-3 ligand (100 ng/ml), human stem cell factor (100 ng/ml), human interleukin (IL)-3 (20 ng/ml), and human IL-6 (20 ng/ml)) (StemCell Technologies Inc., Vancouver, BC, Canada), and were seeded into a 48- or 96-well plate ($1–5 \times 10^4$ cells/well). The cells were transduced with the GFP-expressing Ad35 vectors at the indicated VP/cell 16–18 h after seeding. At 6 h after incubation, the cells were washed to remove the Ad35 vectors and resuspended in the medium. At 48 h after transduction, 10^4 cells per sample were analyzed for GFP expression by flow cytometry on a FACSCalibur flow cytometer using CellQuest software (Becton Dickinson, Tokyo, Japan).

Flow-cytometric analysis of CD46 expression

Human bone marrow CD34$^+$ cells were suspended in staining buffer containing fluorescein isothiocyanate (FITC)-conjugated mouse anti-human CD46 antibody (Pharmingen, San Diego, CA, USA). After washing with the sorting solution, the stained cells (10^4 cells) were analyzed using a FACSCalibur and CellQuest software (Becton Dickinson). For simultaneous analysis of GFP and CD46 expression, the transduced cells were incubated with mouse anti-human CD46 antibody (Pharmingen). Subsequently, the cells were washed and incubated with phycoerythrin (PE)-conjugated goat anti-mouse IgG second antibody (Pharmingen). After washing with the sorting solution, the analysis was performed as described above.

Real-time quantitative PCR

Human bone marrow CD34$^+$ cells were incubated with the Ad35 vectors at 6000 VP/cell, and control cells were incubated without the Ad35 vectors. After a 6-h incubation, the medium was changed to remove the Ad35 vectors. At 48 h after transduction, the cells were harvested, pelleted, and washed gently. The cells were then sorted into GFP-positive and -negative fractions using a FACSVantage SE (Becton Dickinson). Sort purities were greater than 90% for both GFP-positive and -negative fractions. The sorted cells were treated with trypsin and DNase, followed by washing to remove the extracellular vector genome. Total DNA, including the Ad35 vector DNA, was extracted from the GFP-positive and -negative cells using a Tissue DNeasy Kit (Qiagen, Valencia, CA, USA). The quantitative real-time PCR was performed with 2.5 ng of sample DNA, 0.5 μM each primer, 0.16 μM TaqMan probe, and 25 μl of TaqMan universal PCR master mix (Applied Biosystems, Foster City, CA, USA) in a final volume of 50 μl using the ABI Prism 7000 sequence detection system (Applied Biosystems). The PCR was initially denatured at 95°C for 10 min and then subjected to cycles of 95°C for 15 s and

60°C for 1 min. The reaction was carried out for 50 cycles. Primers for amplification were located in the pIX region of Ad35 genome. The sequences of the primers and probe used were as follows: forward, 5′-TGGATGGAAG ACCCGTTCAA-3′; reverse, 5′-CGTCCAAAGGTGAAG AACTTAAAGT-3′; probe, 5′-FAM-CGCCAATTCTTC AACGCTGACCTATGC-TAMRA-3′. These sequences were designed using Primer Express softeware version 1.0 (Applied Biosystems), and it was confirmed that they amplified the products of desired size. The Ad35 vector plasmid pAdMS4 was used as a standard. For human β-actin quantification, β-actin control reagent (Applied Biosystems) was used.

Purification of immature CD34⁺ subpopulations

Human bone marrow $CD34^+$ cells were incubated with PE-conjugated mouse anti-human AC133 monoclonal antibody (Miltenyi Biotec, Bergisch Gladbach, Germany) or FITC-conjugated mouse anti-human CD38 monoclonal antibody (eBioscience, San Diego, CA, USA) immediately after the cells were recovered from the frozen stock. After washing, cell sorting was performed using a FACSVantage SE (Becton Dickinson). Sorting gates were set to sort the $CD38^{low/-}$ and $AC133^+$ subpopulations. Sort purities were greater than 80% for both $CD38^{low/-}$ and $AC133^+$ subpopulations. The sorted $CD34^+CD38^{low/-}$ and $CD34^+AC133^+$ cells were transduced with the Ad35 vectors at 6000 VP/cell, as described above.

Colony-forming assay

The GFP-positive and -negative cells were recovered 48 h after transduction with the Ad35 vector containing the CA promoter, as described above. In all, 1000 cells of each fraction were then plated in a 35-mm dish containing Methocult H4444 methylcellulose medium (erythropoietin; 3 U/ml, stem cell factor; 50 ng/ml, GM-CSF; 10 ng/ml, IL-3; 10 ng/ml) (Stem Cell Technologies). After 14 days of incubation at 37°C in a 5% CO_2 incubator, CFU-GM, BFU-E, and CFU-Mix colonies were enumerated under a microscope. The experiments were performed in duplicate. Uninfected cells were also sorted into a GFP-negative fraction and treated as described above.

Acknowledgements

We thank Tomomi Sasaki and Takashi Fukushima for technical assistance. We would also like to thank Dr J Miyazaki and Dr RG Hawley for kindly providing the CA promoter and the MSCV promoter, respectively. This work was supported in part by a Grants-in-Aid for Scientific Research from the Ministry of Education, Culture, Sports, Science, and Technology of Japan, and by grants for Health and Labour Sciences Research from the Ministry of Health, Labour, and Welfare of Japan.

References

1 Dao MA, Shah AJ, Crooks GM, Nolta JA. Engraftment and retroviral marking of CD34+ and CD34+CD38− human hematopoietic progenitors assessed in immune-deficient mice. *Blood* 1998; **91**: 1243–1255.

2 Orlic D *et al*. The level of mRNA encoding the amphotropic retrovirus receptor in mouse and human hematopoietic stem cells is low and correlates with the efficiency of retrovirus transduction. *Proc Natl Acad Sci USA* 1996; **93**: 11097–11102.

3 Sirven A *et al*. Enhanced transgene expression in cord blood CD34(+)-derived hematopoietic cells, including developing T cells and NOD/SCID mouse repopulating cells, following transduction with modified trip lentiviral vectors. *Mol Ther* 2001; **3**: 438–448.

4 Kahn J *et al*. Overexpression of CXCR4 on human CD34+ progenitors increases their proliferation, migration, and NOD/SCID repopulation. *Blood* 2004; **103**: 2942–2949.

5 Shayakhmetov DM, Papayannopoulou T, Stamatoyannopoulos G, Lieber A. Efficient gene transfer into human CD34(+) cells by a retargeted adenovirus vector. *J Virol* 2000; **74**: 2567–2583.

6 Yotnda P *et al*. Efficient infection of primitive hematopoietic stem cells by modified adenovirus. *Gene Therapy* 2001; **8**: 930–937.

7 Rebel VI *et al*. Maturation and lineage-specific expression of the coxsackie and adenovirus receptor in hematopoietic cells. *Stem Cells* 2000; **18**: 176–182.

8 Takahashi T *et al*. A potential molecular approach to *ex vivo* hematopoietic expansion with recombinant epidermal growth factor receptor-expressing adenovirus vector. *Blood* 1998; **91**: 4509–4515.

9 Segerman A, Mei YF, Wadell G. Adenovirus types 11p and 35p show high binding efficiencies for committed hematopoietic cell lines and are infective to these cell lines. *J Virol* 2000; **74**: 1457–1467.

10 Sakurai F, Mizuguchi H, Hayakawa T. Efficient gene transfer into human CD34+ cells by an adenovirus type 35 vector. *Gene Therapy* 2003; **10**: 1041–1048.

11 Gaggar A, Shayakhmetov DM, Lieber A. CD46 is a cellular receptor for group B adenoviruses. *Nat Med* 2003; **9**: 1408–1412.

12 Segerman A *et al*. Adenovirus type 11 uses CD46 as a cellular receptor. *J Virol* 2003; **77**: 9183–9191.

13 Johnstone RW, Loveland BE, McKenzie IF. Identification and quantification of complement regulator CD46 on normal human tissues. *Immunology* 1993; **79**: 341–347.

14 Liszewski MK, Post TW, Atkinson JP. Membrane cofactor protein (MCP or CD46): newest member of the regulators of complement activation gene cluster. *Annu Rev Immunol* 1991; **9**: 431–455.

15 Manchester M *et al*. Targeting and hematopoietic suppression of human CD34+ cells by measles virus. *J Virol* 2002; **76**: 6636–6642.

16 Fan X, Brun A, Karlsson S. Adenoviral vector design for high-level transgene expression in primitive human hematopoietic progenitors. *Gene Therapy* 2000; **7**: 2132–2138.

17 Byk T, Haddada H, Vainchenker W, Louache F. Lipofectamine and related cationic lipids strongly improve adenoviral infection efficiency of primitive human hematopoietic cells. *Hum Gene Ther* 1998; **9**: 2493–2502.

18 Frey BM *et al*. High-efficiency gene transfer into *ex vivo* expanded human hematopoietic progenitors and precursor cells by adenovirus vectors. *Blood* 1998; **91**: 2781–2792.

19 Ramezani A, Hawley TS, Hawley RG. Lentiviral vectors for enhanced gene expression in human hematopoietic cells. *Mol Ther* 2000; **2**: 458–469.

20 Mizuguchi H, Kay MA. Efficient construction of a recombinant adenovirus vector by an improved *in vitro* ligation method. *Hum Gene Ther* 1998; **9**: 2577–2583.

21 Mizuguchi H, Kay MA. A simple method for constructing E1- and E1/E4-deleted recombinant adenoviral vectors. *Hum Gene Ther* 1999; **10**: 2013–2017.

22 Krougliak V, Graham FL. Development of cell lines capable of complementing E1, E4, and protein IX defective adenovirus type 5 mutants. *Hum Gene Ther* 1995; **6**: 1575–1586.

23 Sakurai F, Mizuguchi H, Yamaguchi T, Hayakawa T. Characterization of *in vitro* and *in vivo* gene transfer properties of adenovirus serotype 35 vector. *Mol Ther* 2003; **8**: 813–821.
24 Foecking MK, Hofstetter H. Powerful and versatile enhancer-promoter unit for mammalian expression vectors. *Gene* 1986; **45**: 101–105.
25 Hao QL *et al*. A functional comparison of CD34 + CD38− cells in cord blood and bone marrow. *Blood* 1995; **86**: 3745–3753.
26 Yin AH *et al*. AC133, a novel marker for human hematopoietic stem and progenitor cells. *Blood* 1997; **90**: 5002–5012.
27 Hao QL *et al*. Extended long-term culture reveals a highly quiescent and primitive human hematopoietic progenitor population. *Blood* 1996; **88**: 3306–3313.
28 Guo ZS, Wang LH, Eisensmith RC, Woo SL. Evaluation of promoter strength for hepatic gene expression *in vivo* following adenovirus-mediated gene transfer. *Gene Therapy* 1996; **3**: 802–810.
29 Xu ZL *et al*. Optimization of transcriptional regulatory elements for constructing plasmid vectors. *Gene* 2001; **272**: 149–156.
30 Cheng L, Ziegelhoffer PR, Yang NS. *In vivo* promoter activity and transgene expression in mammalian somatic tissues evaluated by using particle bombardment. *Proc Natl Acad Sci USA* 1993; **90**: 4455–4459.
31 Ponder KP *et al*. Evaluation of relative promoter strength in primary hepatocytes using optimized lipofection. *Hum Gene Ther* 1991; **2**: 41–52.
32 Lizee G, Gonzales MI, Topalian SL. Lentivirus vector-mediated expression of tumor-associated epitopes by human antigen presenting cells. *Hum Gene Ther* 2004; **15**: 393–404.
33 Kiwaki K *et al*. Correction of ornithine transcarbamylase deficiency in adult spf(ash) mice and in OTC-deficient human hepatocytes with recombinant adenoviruses bearing the CAG promoter. *Hum Gene Ther* 1996; **7**: 821–830.
34 Okabe M *et al*. 'Green mice' as a source of ubiquitous green cells. *FEBS Lett* 1997; **407**: 313–319.
35 Araki K *et al*. Efficiency of recombination by Cre transient expression in embryonic stem cells: comparison of various promoters. *J Biochem (Tokyo)* 1997; **122**: 977–982.
36 Kawabata K *et al*. Efficient gene transfer into mouse embryonic stem cells with adenovirus vectors. *Mol Ther* (in press).
37 Chung S *et al*. Analysis of different promoter systems for efficient transgene expression in mouse embryonic stem cell lines. *Stem Cells* 2002; **20**: 139–145.
38 Sirena D *et al*. The human membrane cofactor CD46 is a receptor for species B adenovirus serotype 3. *J Virol* 2004; **78**: 4454–4462.
39 Schroers R *et al*. Gene transfer into human T lymphocytes and natural killer cells by Ad5/F35 chimeric adenoviral vectors. *Exp Hematol* 2004; **32**: 536–546.
40 Anderson BD, Nakamura T, Russell SJ, Peng KW. High CD46 receptor density determines preferential killing of tumor cells by oncolytic measles virus. *Cancer Res* 2004; **64**: 4919–4926.
41 Segerman A *et al*. There are two different species B adenovirus receptors: sBAR, common to species B1 and B2 adenoviruses, and sB2AR, exclusively used by species B2 adenoviruses. *J Virol* 2003; **77**: 1157–1162.
42 Jin CH *et al*. Recombinant Sendai virus provides a highly efficient gene transfer into human cord blood-derived hematopoietic stem cells. *Gene Therapy* 2003; **10**: 272–277.
43 Knaan-Shanzer S *et al*. Highly efficient targeted transduction of undifferentiated human hematopoietic cells by adenoviral vectors displaying fiber knobs of subgroup B. *Hum Gene Ther* 2001; **12**: 1989–2005.
44 Dorrell C *et al*. Expansion of human cord blood CD34(+)CD38(−) cells in *ex vivo* culture during retroviral transduction without a corresponding increase in SCID repopulating cell (SRC) frequency: dissociation of SRC phenotype and function. *Blood* 2000; **95**: 102–110.
45 Donaldson C, Denning-Kendall P, Bradley B, Hows J. The CD34(+)CD38(neg) population is significantly increased in haemopoietic cell expansion cultures in serum-free compared to serum-replete conditions: dissociation of phenotype and function. *Bone Marrow Transplant* 2001; **27**: 365–371.
46 Mizuguchi H, Kay MA, Hayakawa T. Approaches for generating recombinant adenovirus vectors. *Adv Drug Deliv Rev* 2001; **52**: 165–176.
47 Seshidhar Reddy P *et al*. Development of adenovirus serotype 35 as a gene transfer vector. *Virology* 2003; **311**: 384–393.
48 Vogels R *et al*. Replication-deficient human adenovirus type 35 vectors for gene transfer and vaccination: efficient human cell infection and bypass of preexisting adenovirus immunity. *J Virol* 2003; **77**: 8263–8271.
49 Gao W, Robbins PD, Gambotto A. Human adenovirus type 35: nucleotide sequence and vector development. *Gene Therapy* 2003; **10**: 1941–1949.
50 Shayakhmetov DM *et al*. A high-capacity, capsid-modified hybrid adenovirus/adeno-associated virus vector for stable transduction of human hematopoietic cells. *J Virol* 2002; **76**: 1135–1143.
51 Ueno T *et al*. Site-specific integration of a transgene mediated by a hybrid adenovirus/adeno-associated virus vector using the Cre/loxP-expression-switching system. *Biochem Biophys Res Commun* 2000; **273**: 473–478.
52 Recchia A *et al*. Site-specific integration mediated by a hybrid adenovirus/adeno-associated virus vector. *Proc Natl Acad Sci USA* 1999; **96**: 2615–2620.
53 Mizuguchi H *et al*. Tight positive regulation of transgene expression by a single adenovirus vector containing the rtTA and tTS expression cassettes in separate genome regions. *Hum Gene Ther* 2003; **14**: 1265–1277.
54 Okada N *et al*. Efficient antigen gene transduction using Arg–Gly–Asp fiber-mutant adenovirus vectors can potentiate anti-tumor vaccine efficacy and maturation of murine dendritic cells. *Cancer Res* 2001; **61**: 7913–7919.

Available online at www.sciencedirect.com

SCIENCE DIRECT®

Journal of Controlled Release 108 (2005) 56–62

journal of controlled release

www.elsevier.com/locate/jconrel

Role of C-terminal regions of the C-terminal fragment of *Clostridium perfringens* enterotoxin in its interaction with claudin-4

Azusa Takahashi [a], Masuo Kondoh [a,*], Akane Masuyama [a], Makiko Fujii [a], Hiroyuki Mizuguchi [b], Yasuhiko Horiguchi [c], Yoshiteru Watanabe [a]

[a] *Department of Pharmaceutics and Biopharmaceutics, Showa Pharmaceutical University, Machida, Tokyo 194-8543, Japan*
[b] *Laboratory of Gene Transfer and Regulation, National Institute of Biomedical Innovation, Osaka 567-0085, Japan*
[c] *Department of Bacterial Toxinology, Division of Infectious Diseases, Osaka University, Osaka 565-0871, Japan*

Received 24 March 2005; accepted 12 July 2005
Available online 8 August 2005

Abstract

Claudin family proteins, which contain 4 transmembrane domains, play a pivotal role in the barrier function of tight junctions (TJs) in epithelial sheets. We previously found that a modulator of claudin-4, the C-terminal fragment of *Clostridium perfringens* enterotoxin (C-CPE), is a potent enhancer of jejunal drug absorption in rats. But the effects of C-CPE on the barrier function of TJs have never been fully understood. In the present study, we investigated the effects of C-CPE on the barrier function of TJs in Caco-2 monolayer and characterized the functional domain of C-CPE that is responsible for interaction with claudin-4. To evaluate the effects of C-CPE on the barrier function of TJs, we measured transepithelial electric resistance (TER) in Caco-2 monolayer cells seeded onto polycarbonate filters. Treatment of Caco-2 cells with C-CPE resulted in a decrease in TER. But, deletion of the 30 C-terminal amino acids of C-CPE, which is the putative binding domain for claudin, attenuated the decrease in TER values. Moreover, ablation of the 16 C-terminal amino acids of C-CPE also resulted in attenuation of the decrease in TER values. The C-terminal-deleted C-CPEs did not interact with claudin-4 or the extracellular domain 2 of claudin-4, which is the C-CPE binding site. These results suggest that the 16 C-terminal amino acids of C-CPE are responsible for the interaction of C-CPE and claudin-4 following the disruption of TJ barrier function.

Keywords: Tight junction; Claudin-4; Caco-2; Transepithelial electric resistance; *Clostridium perfringens* enterotoxin

1. Introduction

Tight junctions (TJs) play a role in paracellular barriers with physiological properties, such as elec-

Abbreviations: CPE, *Clostridium perfringens* enterotoxin; C-CPE, C-terminal fragment of *Clostridium perfringens* enterotoxin; TER, transepithelial electric resistance; EC2hcld-4, extracellular domain 2 of human claudin-4.

* Corresponding author. Tel.: +81 42 721 1556; fax: +81 42 723 3585.
E-mail address: masuo@ac.shoyaku.ac.jp (M. Kondoh).

0168-3659/$ - see front matter © 2005 Elsevier B.V. All rights reserved.
doi:10.1016/j.jconrel.2005.07.008

trical resistance and discrimination of solute size and charge, which differ among tissues [1]. Recent progress in the cell biology of TJs provides evidence that a family of transmembrane proteins called the claudins regulates the barrier function of TJs [1–3].

Claudin is a ~23 kDa integral membrane protein with 4 transmembrane domains, and the claudins comprise a multigene family with more than 20 members [3]. Claudin family members are expressed in a tissue-specific manner. Claudin-1 and -2 are highly expressed in liver and kidney. Claudin-5 is localized in endothelial cells. Claudin-11 expression is observed in brain and testis [4–7]. The barrier functions of claudins in tight junctions differ among tissues. Claudin-1, a component of tight junctions in the epidermis, is crucial for the epidermal barrier. A tracer with a molecular weight of ~600 Da passes through the epidermis in claudin-1-deficient mice [8]. Claudin-5 deficiency allows small molecules (<800 Da) to cross the blood–brain barrier [9]. Paracellular transport of ions across epithelia is regulated by expression profiles of claudins [10]. If we can establish a method to modulate the barrier function of claudin in a claudin family member-specific manner, the method would be useful for basic research to clarify the biological function of claudin in TJs. This method would also have an important clinical application for tissue-specific drug delivery.

Clostridium perfringens enterotoxin (CPE), a single polypeptide with a molecular weight of ~35 kDa, is the causative agent of *C. perfringens* food poisoning in humans [11]. The first step in the poisoning mechanism is the binding of CPE to its receptors on the cell membrane. Receptor binding is followed by the formation of a small complex and the subsequent formation of a large complex. The formation of the small complex is not cytotoxic, but the formation of the large complex is cytotoxic [12]. The binding of CPE to the mucosal membrane in the intestine is believed to be mediated by the 30 C-terminal amino acids of C-CPE, while the formation of the large complex (and the subsequent cytotoxicity) is mediated by the N-terminal domain [12,13]. Claudin-3 and -4 are receptors for CPE [14,15]. Interestingly, the treatment of cells with the C-terminal fragment of CPE184-319 (C-CPE) results in decreased claudin-4 protein levels and disruption of the TJ barrier without any cytotoxicity [15]. These reports indicate that the identification of the essential domain in C-CPE for binding to claudin-4 would be useful for the development of a targeting molecule against other claudin family members.

In the present study, we characterized a role for the of C-terminal domain of C-CPE in the binding of C-CPE to claudin-4 and the disruption of TJ barriers in Caco-2 cells, which are used as a cell culture model of intestinal epithelial cells [16–19]. We found that the 16 C-terminal amino acids of C-CPE are responsible for biological activities, including affinity for claudin-4 and attenuation of TJ barrier function.

2. Materials and methods

2.1. Cell cultures

Caco-2, a human intestinal cell line, was maintained in DMEM medium containing 10% fetal bovine serum in a 5% CO_2 atmosphere at 37 °C. Cells from passages 60 through 65 were used for experiments.

2.2. Preparation of C-CPE and C-terminal-deleted C-CPE

We prepared C-CPE, C-CPE289 (which lacks 30 C-terminal amino acids), and C-CPE303 (which lacks 16 C-terminal amino acids) as described previously [20]. Briefly, a plasmid encoding histidine-fused C-CPE, C-CPE289, or C-CPE303 was transduced into *E. coli* BL21 (DE3) strains (Novagen, Darmstadt, Germany). Production of the C-CPEs was induced by the addition of isopropyl-1-thio-β-D-galactoside into the culture medium. The cells were lysed and centrifuged. The resultant supernatant was applied to a column filled with Ni-resin (Invitrogen, Gaithersburg, MD). The C-CPEs were eluted by imidazole, and the solvent was changed to phosphate buffered saline (PBS) using PD-10 columns (Amersham, Piscataway, NJ). The concentration of C-CPEs was determined with a commercially available protein assay kit using serum albumin as a protein standard (Bio-Rad, Hercules, CA).

2.3. Measurement of transepithelial electric resistance

Confluent monolayers of Caco-2 cells were grown in Transwell chambers. The formation of TJ barriers in Caco-2 monolayers was monitored by measuring the transepithelial electric resistance (TER) using a Millicell-ERS epithelial volt-ohmmeter (Millipore Co.). After 10–14 days of culture, the TER values reached a plateau. Then, the TJ-developing cells were used for experiments. Caco-2 monolayer cells were treated with C-CPE on the apical side of the chamber, and then TER values were measured. The TER values were normalized by the area of the Caco-2 monolayer. The background TER of a blank Transwell chamber was subtracted from the TER of cell monolayers.

2.4. Interaction of C-CPEs with claudin-4 in Caco-2 lysates

Confluent Caco-2 cells were harvested and lysed in lysis buffer (1% Triton X-100, 0.2% SDS, 150 mM NaCl, 10 mM HEPES (pH 7.4), 2 mM EDTA, and 1% protease inhibitor cocktail (Sigma, St Louis, MO)). C-CPEs were incubated with the lysates for 2 h at 4 °C, and then Ni-resin beads were added. After an additional 2 h of incubation at 4 °C, the beads were washed with the lysis buffer. The beads were subjected to SDS-PAGE followed by Western blotting. Anti-human claudin-4 Ab (Zymed Laboratories, San Francisco, CA) and anti-His tag Ab (Novagen) were used to detect claudin-4 and the C-CPE proteins, respectively. The bound primary antibody was detected by peroxidase-labeled secondary antibody using chemiluminescence reagents (Amersham Bioscience, NJ).

2.5. Preparation of recombinant EC2hcld-4

We subcloned the extracellular domain 2 of human claudin-4 (EC2hcld-4) (141 aa–210 aa) using a human placenta cDNA library (TaKaRa, Shiga, Japan) as a template. The template was subjected to PCR using gaattccacaacatcatccaagacttctac as the sense primer and aagcttacacgtagttgctggcagc as the antisense primer. The resultant EC2hcld-4 fragments were subcloned into pGEM®T-Easy vector (Promega, Madison, WI). The EcoRI/NotI-digested pGEM®T-Easy vector containing EC2hcld-4 products was inserted into the similarly digested pGEX4T-1 plasmid (Amersham BioScience). This process resulted in an expression vector of glutathione *S*-transferase (GST)-fused EC2hCld-4 (GST/EC2hcld-4). GST/EC2hcld-4 was purified as described previously [21]. Briefly, pGEX4T-1 plasmid with EC2hcld-4 was introduced into the *E. coli* BL21 (DE3) strain, and expression of the GST/EC2hCld-4 was induced by isopropyl β-D-thiogalactopyranoside. *Escherichia coli* was lysed in STE buffer (10 mM Tris-HCl (pH 8.0), 150 mM NaCl, 1 mM EDTA) containing 100 μg/ml lysozyme, 5 mM dithiothreitol, and 1.5% *N*-lauroylsarcosine. The lysates were centrifuged, and the resultant supernatant was treated with 2% Triton X-100 followed by incubation with glutathione-agarose beads for 2 h at 4 °C. Then the beads were washed with STE buffer, and the GST/EC2hCld-4 bound to the beads was eluted with STE buffer containing 50 mM glutathione. The buffer of the GST/EC2hCld-4 solution was exchanged with PBS using PD-10 columns (Amersham Bioscience). Preparation of GST/EC2hCld-4 was confirmed by SDS-PAGE followed by staining the gels with Coomassie Brilliant Blue and by Western blotting with a GST-tagged antibody (data not shown).

2.6. Interaction of C-CPEs with extracellular domain 2 of claudin-4

Immunoplates (Nunc, Roskilde, Denmark) were coated with 10 μg/ml GST or GST/EC2hCld-4 in 50 mM bicarbonate buffer. The wells were washed with T-TBS (20 mM Tris-HCl pH 7.4, 40 mM NaCl, 0.05% Tween-20), and then the wells were blocked with 1% gelatin in TBS (20 mM Tris–HCl pH 7.4, 40 mM NaCl) for 2 h at room temperature. The wells were washed with T-TBS, and then the wells were incubated with C-CPEs at the indicated concentrations for 2 h at room temperature. Then, the wells were incubated with anti-His tag antibody (Novagen, Darmstadt, Germany) for 2 h at room temperature. The wells were then treated with horseradish peroxidase-labeled antibody for 2 h at room temperature. Ten minutes after addition of 55 mM 3,3′, 5,5′-tetramethylbenzidinethe in dimethylformamide, color development was terminated by addition of 2 N H_2SO_4. The reacted product was detected by spectrometry at 450 nm. Background reactivity due to non-specific binding of secondary antibodies was

subtracted from reactivity observed in the presence of primary antibodies.

2.7. Statistical analysis

Statistical analysis was performed using one-way ANOVA followed by Dunnett's method. The level of significance was set at $p<0.05$.

3. Results

3.1. Effects of C-terminal region-deleted C-CPEs on TJ barriers

The 30 C-terminal amino acids of CPE, the region between 289 aa and 319 aa, is responsible for interaction with its receptor [13]. Therefore, we focused on the C-terminal region in the present study. To evaluate the function of the C-terminal region of C-CPE on TJ barrier function, we prepared C-CPE289 and C-CPE303, which contain a 30 amino acid deletion

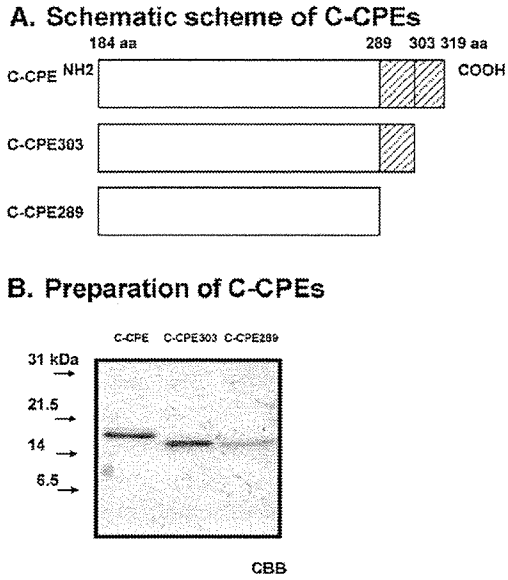

Fig. 1. Preparation of C-CPEs. (A) C-CPE, C-CPE303, and C-CPE289. C-CPE is the C-terminal fragment of CPE between 184 aa and 319 aa [14]. The shaded area (290 aa–319 aa) indicates the putative receptor binding site [13]. (B) Preparation of C-CPE, C-CPE303, and C-CPE289. C-CPE, C-CPE303, and C-CPE289 were purified and subjected to SDS-PAGE followed by staining with Coomassie Brilliant Blue (CBB).

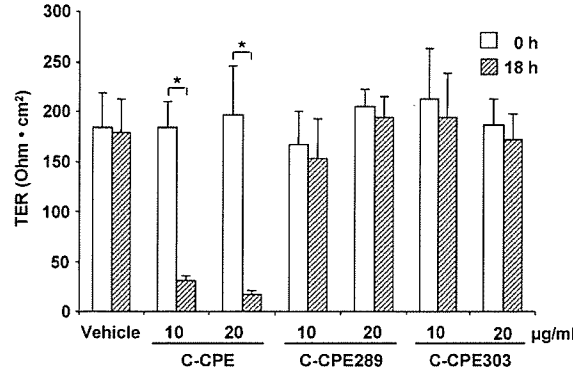

Fig. 2. Effects of C-CPEs on transepithelial electric resistance (TER) in Caco-2 monolayer cells. Confluent Caco-2 cells were cultured for 10–14 days. When TER values were constant, each C-CPE was added to the basal side in Transwell chambers at the indicated concentrations. After 18 h of incubation, TER values were measured. Data are means ± SD ($n=4$). *Significant difference between 0 h and 18 h.

(between 290 aa and 319 aa) and a 16 amino acid deletion (between 304 aa and 319 aa), respectively (Fig. 1A). C-CPEs were fused to 10 consecutive histidine residues to facilitate purification. The purified C-CPEs were confirmed by SDS-PAGE followed by staining with Coomassie brilliant blue and Western blotting (Fig. 1B, data not shown). To evaluate the influence of C-CPEs on TJ barrier function, we measured changes in TER values, an indication of TJ barrier function, in Caco-2 monolayer cells that were seeded onto polycarbonate filters and treated with C-CPEs. Although apical addition of C-CPE did not change TER values, basal addition of C-CPE resulted in a time- and dose-dependent decrease in TER values (Fig. 2). TER values decreased from $183.7 \pm 26.4\ \Omega\ cm^2$ to $30.3 \pm 4.9\ \Omega\ cm^2$ after 18-h treatment with C-CPE (10 μg/ml). On the contrary, decreases in TER values were not observed after apical or basal treatment with C-CPE289 or C-CPE303 (10 μg/ml) for 18 h.

3.2. Interaction of C-CPEs with claudin-4

Claudin-4 is a receptor for CPE, and claudin-4 plays a pivotal role in the maintenance of TJ barrier function [12,15]. Next, we evaluated the interaction of C-CPEs and claudin-4. After incubation of C-CPEs (10 μg of protein) and Caco-2 lysates (100 μg of protein), Ni-resin was added to the mixture and the resins were precipitated. Claudin-4 was precipitated

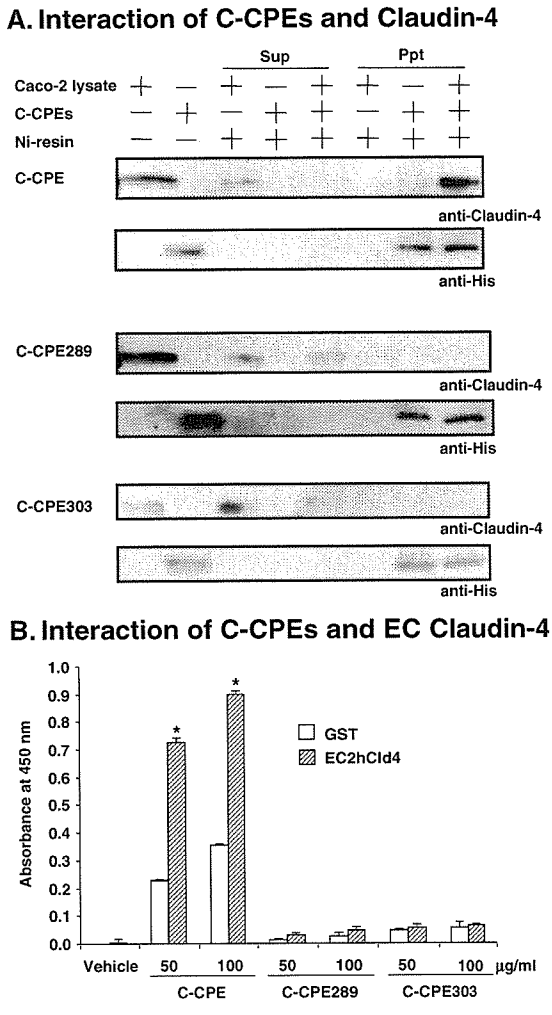

Fig. 3. Interaction of C-CPEs with claudin-4. (A) Interaction of C-CPEs with claudin-4 in Caco-2 lysates. Confluent Caco-2 cells were harvested and lysed in lysis buffer. The lysate (10 μg) was incubated with vehicle or C-CPEs for 2 h at 4 °C. Ni-resin was added. After an additional 2 h of incubation at 4 °C, the resin was precipitated and the resultant precipitation and the supernatant were subjected to SDS-PAGE followed by Western blotting. (B) Interaction of C-CPEs with EC2hCld-4. Immunoplates were coated with GST or GST/EC2hCld-4 (10 μg/ml). After blocking the plates with skim milk, the wells were treated with C-CPEs at the indicated concentration for 2 h at room temperature. Then, the wells were incubated with anti-His tagged Ab followed by incubation with peroxide-labeled Ab. The peroxide-labeled Ab was detected using 3,3′,5,5′-tetramethylbenzidinethe as a substrate. Data are means ± SD (n=4). *Significant difference between GST- and GST/EC2hCld-4-coated wells.

by Ni-resin in Caco-2 lysates incubated with C-CPE (10 μg/ml) (Fig. 3A). But, incubation of C-CPE303 or C-CPE289 with Caco-2 lysates did not result in precipitation of claudin-4 by Ni-resin (Fig. 3A), indicating that the C-terminal region of C-CPE between 303 and 319 aa may be responsible for interaction with claudin-4. C-CPE interacts with extracellular domain 2 of claudin [22]. So, to confirm the interaction between C-CPEs and claudin-4, we prepared glutathione *S*-transferase-fused extracellular domain 2 of claudin-4 protein (GST/EC2hCld-4) and performed ELISA assays using GST or GST/EC2hCld-4 protein as a coating protein. C-CPE interacted with EC2hCld-4 in a dose-dependent fashion, but C-CPE289 and C-CPE303 did not interact with EC2hCld-4. Taken together, these results indicate that the 16 C-terminal amino acids may be critical for the binding of C-CPE to claudin-4.

4. Discussion

C-CPE is a novel and potent enhancer of drug absorption due to its interaction with claudin-4; C-CPE enhances drug absorption by over 400-fold when compared to a clinically used enhancer [20]. In the present study, we characterized the role of the C-terminal region of C-CPE in disrupting TJ barrier function and interacting with claudin-4. We found that the 16 C-terminal amino acids of C-CPE were responsible for these functions.

McClane et al. characterized CPE receptors and the functional receptor-binding domain of CPE (reviewed in [12]). They classified CPE receptors into two types: a ~22 kDa protein and a ~45–50 kDa protein. The larger receptor is part of the small protein complex that has a molecular mass of ~90 kDa; the small protein complex results in the formation of a large complex (with a molecular weight of >150 kDa) on the cell membrane. The 22 kDa receptor is believed to be claudin-4 [12,15]. Hanna et al. (1991) found that the 30 C-terminal amino acids of CPE were responsible for its binding to a receptor in rabbit intestinal membrane; but this CPE receptor was not identified [13]. In the current study, we found that the 30 C-terminal amino acids of C-CPE are responsible for its interaction with claudin-4. This result is consistent with a past report [12,15]. Additional analysis of the

C-terminal region of C-CPE provided us with the new insight that the 16 C-terminal amino acids of C-CPE may be essential for its interaction with claudin-4. The expression of claudin protein is up-regulated in some tumors, and claudin is a novel targeting molecule for pancreatic tumors and prostate cancer [23–25]. Thus, a claudin-based drug delivery system may enhance the delivery of chemotherapy drugs to tumors. The present data regarding the functional claudin-4 binding regions of C-CPE will be important for the development of a drug delivery system that targets claudin with some modification of the claudin-4-binding site of C-CPE.

In the present report, we show that C-CPE disrupts the TJ barrier function. This result is consistent with a past report that treatment of MDCK cells with C-CPE disrupted TJ barrier function [15]. We previously found that deletion of the C-terminal region C-CPE attenuated the enhancement of jejunal drug absorption [20]. In the present study, we also found that the 16 C-terminal amino acids of C-CPE are responsible for the disruption of the TJ barrier function in Caco-2 monolayer cells. Thus, the absorption-enhancing effects of C-CPE may be due to the disruption of the TJ barrier function that is triggered by the interaction of claudin-4 and C-CPE. TJs are localized on the apical side of intercellular junctions, but treatment of the Caco-2 cells with C-CPE on the apical side did not disrupt TJ barriers (data not shown). However, treatment of the cells with C-CPE on the basal side resulted in decreased TJ barrier function. Similar results were observed in MDCK cells, as well as in a study of the cytotoxicity of C-CPE in Caco-2 cells [15,26]. The precise mechanism responsible for the polarity of the effects of C-CPE on the TJ barrier is still unclear. Elucidation of the polarity issue will clarify the mechanism by which C-CPE disrupts TJ barrier function, as well as the biological significance of claudin.

In summary, we found that C-CPE may be a potent modulator of claudin because modification of 16 C-terminal amino acids in C-CPE may be a useful approach to prepare a modulator of another claudin family protein. The elucidation of this mechanism will result in an understanding of claudin's role in the TJ barrier function, as well as the potential to produce a tissue-specific drug delivery system (via the paracellular pathway) that is dependent on the modulation of TJs. This is the first report to indicate that the C-terminal region of C-CPE disrupts TJ barrier function.

Acknowledgements

We thank Mr. M. Harada and Mr. N. Koizumi for their excellent technical support. This study is partly supported by a Grant-in-Aid of the Ministry of Education, Sports and Science in Japan.

References

[1] J.M. Anderson, Molecular structure of tight junctions and their role in epithelial transport, News Physiol. Sci. 16 (2001) 126–130.
[2] S. Tsukita, M. Furuse, Pores in the wall: claudins constitute tight junction strands containing aqueous pores, J. Cell Biol. 149 (2000) 13–16.
[3] S. Tsukita, M. Furuse, M. Itoh, Multi-functional strands in tight junctions, Nat. Rev., Mol. Cell Biol. 2 (2001) 285–293.
[4] M. Furuse, K. Fujita, T. Hiiragi, K. Fujimoto, S. Tsukita, Claudin-1 and -2: novel integral membrane proteins localizing at tight junctions with no sequence similarity to occludin, J. Cell Biol. 141 (1998) 1539–1550.
[5] K. Morita, H. Sasaki, M. Furuse, S. Tsukita, Endothelial claudin: claudin-5/TMVCF constitutes tight junction strands in endothelial cells, J. Cell Biol. 147 (1999) 185–194.
[6] K. Morita, H. Sasaki, K. Fujimoto, M. Furuse, S. Tsukita, Claudin-11/OSP-based tight junctions of myelin sheaths in brain and Sertoli cells in testis, J. Cell Biol. 145 (1999) 579–588.
[7] A. Hellani, J. Ji, C. Mauduit, C. Deschildre, E. Tabone, M. Benahmed, Developmental and hormonal regulation of the expression of oligodendrocyte-specific protein/claudin 11 in mouse testis, Endocrinology 141 (2000) 3012–3019.
[8] M. Furuse, M. Hata, K. Furuse, Y. Yoshida, A. Haratake, Y. Sugitani, T. Noda, A. Kubo, S. Tsukita, Claudin-based tight junctions are crucial for the mammalian epidermal barrier: a lesson from claudin-1-deficient mice, J. Cell Biol. 156 (2002) 1099–1111.
[9] T. Nitta, M. Hata, S. Gotoh, Y. Seo, H. Sasaki, N. Hashimoto, M. Furuse, S. Tsukita, Size-selective loosening of the blood–brain barrier in claudin-5-deficient mice, J. Cell Biol. 161 (2003) 653–660.
[10] C.M. Van Itallie, A.S. Fanning, J.M. Anderson, Reversal of charge selectivity in cation or anion-selective epithelial lines by expression of different claudins, Am. J. Physiol. 285 (2003) F1078–F1084.
[11] B.A. McClane, P.C. Hanna, A.P. Wnek, *Clostridium perfringens* enterotoxin, Microb. Pathog. 4 (1988) 317–323.
[12] B.A. McClane, G. Chakrabarti, New insights into the cytotoxic mechanisms of *Clostridium perfringens* enterotoxin, Anaerobe 10 (2004) 107–114.

[13] P.C. Hanna, T.A. Mietzner, G.K. Schoolnik, B.A. McClane, Localization of the receptor-binding region of *Clostridium perfringens* enterotoxin utilizing cloned toxin fragments and synthetic peptides, J. Biol. Chem. 266 (1991) 11037–11043.
[14] J. Katahira, N. Inoue, Y. Horiguchi, M. Matsuda, N. Sugimoto, Molecular cloning and functional characterization of the receptor for *Clostridium perfringens* enterotoxin, J. Cell Biol. 136 (1997) 1239–1247.
[15] N. Sonoda, M. Furuse, H. Sasaki, S. Yonemura, J. Katahira, Y. Horiguchi, S. Tsukita, *Clostridium perfringens* enterotoxin fragment removes specific claudins from tight junction strands: evidence for direct involvement of claudins in tight junction barrier, J. Cell Biol. 147 (1999) 195–204.
[16] J.H. Hochman, J.A. Fix, E.L. LeCluyse, In vitro and in vivo analysis of the mechanism of absorption enhancement by palmitoylcarnitine, J. Pharmacol. Exp. Ther. 269 (1994) 813–822.
[17] T. Lindmark, T. Nikkila, P. Artursson, Mechanism of absorption enhancement by medium chain fatty acids in intestinal epithelial Caco-2 cell monolayers, J. Pharmacol. Exp. Ther. 275 (1995) 958–964.
[18] M. Tomita, M. Hayashi, S. Awazu, Absorption-enhancing mechanism of sodium caprate and decanoylcarnitine in Caco-2 cells, J. Pharmacol. Exp. Ther. 272 (1995) 739–743.
[19] W.C. Yen, V.J.L. Lee, Role of Na^+ in asymmetric paracellular transport of 4-phenylazobenzyloxycarbonyl-L-Pro-L-Leu-Gly-L-Pro-D-Arg across rabbit colonic segments and Caco-2 cell monolayer, J. Pharmacol. Exp. Ther. 275 (1995) 114–119.
[20] M. Kondoh, A. Masuyama, A. Takahashi, N. Asano, H. Mizuguchi, N. Koizumi, M. Fujii, T. Hayakawa, Y. Horiguchi, Y. Watanabe, A novel strategy for the enhancement of drug absorption using a claudin modulator, Mol. Pharmacol. 67 (2005) 749–756.
[21] J.V. Frangioni, B.G. Neel, Solubilization and purification of enzymatically active glutathione *S*-transferase (pGEX) fusion proteins, Anal. Biochem. 210 (1993) 179–187.
[22] K. Fujita, J. Katahira, Y. Horiguchi, N. Sonoda, M. Furuse, S. Tsukita, *Clostridium perfringens* enterotoxin binds to the second extracellular loop of claudin-3, a tight junction integral membrane protein, FEBS Lett. 476 (2000) 258–261.
[23] P. Michl, M. Buchholz, M. Rolke, S. Kunsch, M. Lohr, B.A. McClane, S. Tsukita, G. Leder, G. Adler, T.M. Gress, Claudin-4: a new target for pancreatic cancer treatment using *Clostridium perfringens* enterotoxin, Gastroenterology 121 (2001) 678–684.
[24] H. Long, C.D. Crean, W.H. Lee, O.W. Cummings, T.G. Gabig, Expression of *Clostridium perfringens* enterotoxin receptors Claudin-3 and Claudin-4 in prostate cancer epithelium, Cancer Res. 61 (2001) 7878–7881.
[25] P. Michl, C. Barth, M. Buchholz, M.M. Lerch, M. Rolke, K.H. Holzmann, A. Menke, H. Fensterer, K. Giehl, M. Lohr, G. Leder, T. Iwamura, G. Adler, T.M. Gress, Claudin-4 expression decreases invasiveness and metastatic potential of pancreatic cancer, Cancer Res. 63 (2003) 6265–6271.
[26] U. Singh, L.L. Mitic, E.U. Wieckowski, J.M. Anderson, B.A. McClane, Comparative biochemical and immunocytochemical studies reveal differences in the effects of *Clostridium perfringens* enterotoxin on polarized Caco-2 cells *versus* Vero cells, J. Biol. Chem. 276 (2001) 33402–33412.

Available online at www.sciencedirect.com
SCIENCE DIRECT®
ELSEVIER
Biochemical and Biophysical Research Communications 332 (2005) 1101–1106
BBRC
www.elsevier.com/locate/ybbrc

Fiber-modified adenovirus vectors mediate efficient gene transfer into undifferentiated and adipogenic-differentiated human mesenchymal stem cells

Hiroyuki Mizuguchi [a,b,*], Tomomi Sasaki [a], Kenji Kawabata [a], Fuminori Sakurai [a], Takao Hayakawa [c]

[a] *Laboratory of Gene Transfer and Regulation, National Institute of Biomedical Innovation, Osaka 567-0085, Japan*
[b] *Graduate School of Pharmaceutical Sciences, Osaka University, Osaka 565-0871, Japan*
[c] *Pharmaceuticals and Medical Devices Agency, Tokyo 100-0013, Japan*

Received 6 May 2005
Available online 23 May 2005

Abstract

Human mesenchymal stem cells (hMSCs) are considered a source of cells for regenerative medicine, and cell and gene therapy. Efficient gene transfer into hMSCs is essential for basic investigations into cellular differentiation and developmental biology, and for therapeutic applications in gene-modified regenerative medicine. In the present study, we optimized the transduction of hMSCs by means of fiber-modified adenovirus (Ad) vectors. Among the various types of Ad vectors tested, the polylysine modification of the C-terminal of the fiber knob most markedly improved the efficiency of hMSC transduction. At 300 vector particles per cell of polylysine-modified Ad vectors, more than 95% of the hMSCs expressed transgene. In this condition, polylysine-modified Ad vectors mediated 460-fold more transgene activity than the conventional Ad vectors. Ad vectors containing the Ad type 35 fiber or an Arg-Gly-Asp (RGD) peptide in the fiber knob mediated 130 or 16 times, respectively, the transgene activity mediated by the conventional Ad vectors. We also examined the efficiency of transduction into adipogenic-differentiated hMSCs. In this latter case, only Ad vectors containing the Ad type 35 fiber showed efficient gene expression. These results showed that fiber-modified Ad vectors could become a potent tool for basic research into, and the therapeutic application of, hMSCs and adipogenic-differentiated hMSCs.

Keywords: Adenovirus vector; Mesenchymal stem cells; Adipocytes; Gene therapy; Regenerative medicine

Bone marrow-derived mesenchymal stem cells (MSCs) have high proliferative capacity [1] and can differentiate into adipocytes, osteoblasts, and chondrocytes [2]. They can also differentiate into other types of cells such as nerve cells [3,4] and hepatocytes [5]. MSCs are considered vehicles for cell and gene therapy. As vehicles for cell therapy, MSCs are directly injected into the mesenchymal tissues, because these cells are progenitors of mesenchymal tissues. As vehicles for gene therapy, genetically modified MSCs are delivered systemically or injected directly to tissues of interest to express therapeutic proteins in the desired tissues. To generate genetically modified MSCs, it is essential to use a vector that efficiently mediates gene transfer into MSCs. An efficient gene transfer vector is also essential for basic research into MSCs, such as analyses of cellular differentiation and developmental biology.

Recombinant adenovirus (Ad) vectors continue to be the preferred vectors for gene therapy and the study of gene function. They are relatively easy to construct, can be produced at high titers, and have high transduction efficiencies. The efficiency of Ad vector-mediated transduction into human MSCs (hMSCs), however, is

* Corresponding author. Fax: +81 72 641 9816.
E-mail address: mizuguch@nibio.go.jp (H. Mizuguchi).

0006-291X/$ - see front matter © 2005 Elsevier Inc. All rights reserved.
doi:10.1016/j.bbrc.2005.05.055

quite low due to the scarcity of the primary receptor, called the coxsackievirus and adenovirus receptor (CAR) [6–9]. Therefore, hMSCs usually have been transduced with high titers (more than 1000 infectious units/cell) of Ad vectors [6,8,9]. Fiber-modified Ad vectors overcome this obstacle. We and other groups have developed several types of fiber-modified Ad vectors. One is constructed by the addition of foreign peptides to the HI loop or C-terminal of the fiber knob of an Ad vector [10–14]. Enhanced gene transfer has been reported, based on the use of mutant fiber proteins containing either an Arg-Gly-Asp (RGD) peptide [10–15] or a stretch of lysine residues (K7 (KKKKKKK) peptide) [10,14,15], which, respectively, target αv integrins or heparan sulfates on the cellular surface. Another type of fiber-modified Ad vector is made by removing fibers from one Ad serotype (Ad type 5) and replacing them with fibers derived from another—specifically, fibers that bind to receptor molecules other than CAR [16–20]. That is, fiber proteins derived from Ad belonging to the subgroup B, such as Ad type 3, 11, and 35, replace the Ad type 5 fiber. These fiber-modified Ad vectors infect cells via CD46, CD80, or CD86, which are recently identified cellular receptors of Ad belonging to subgroup B [21–25].

In the present study, we optimized the transduction to hMSCs by Ad vectors containing an RGD peptide in the HI loop of the fiber knob, Ad vectors containing a polylysine peptide in the C-terminal of the fiber knob, and Ad vectors containing a fiber protein derived from the Ad type 5 fiber tail, and the Ad type 35 fiber knob and shaft. The results showed that polylysine modification of the fiber knob greatly improved the efficiency of Ad vector-mediated transduction into hMSCs. We also report the efficient gene transfer into adipogenic-differentiated hMSCs by the Ad vectors containing Ad type 35 fiber.

Materials and methods

Ad vectors. Ad vectors expressing an *Escherichia coli* β-galactosidase (LacZ) were constructed by an improved in vitro ligation method [26,27]. The shuttle plasmid pHMCA-LacZ1 contains a CA promoter (a β-actin promoter/CMV enhancer with a β-actin intron) [this promoter/enhancer was kindly provided by Dr. J. Miyazaki (Osaka University, Osaka, Japan)] [28], the LacZ gene derived from pCMVβ (Clontech, Palo Alto, CA, USA), and a bovine growth hormone polyadenylation signal, all of which are flanked by I-CeuI and PI-SceI sites. I-CeuI/PI-SceI-digested pHMCA-LacZ1 was ligated with I-CeuI/PI-SceI-digested pAdHM4 [26], resulting in pAdHM4-CALacZ1. pAdHM15-RGD-CALacZ1, pAdHM41-K7-CALacZ1, and pAdHM34-CALacZ1 were constructed by the ligation of I-CeuI/PI-SceI-digested pHMCA-LacZ1 with I-CeuI/PI-SceI-digested pAdHM15-RGD [13], pAdHM41-K7 [14], and pAdHM34 [20], respectively. Viruses (Ad-CALacZ, AdRGD-CALacZ, AdK7-CALacZ, and AdF35-CALacZ) were generated with the transfection of PacI-digested pAdHM4-CALacZ1, pAdHM15-RGD-CALacZ1, pAdHM41-K7-CALacZ1, and pAdHM34-CALacZ1, respectively, into 293 cells per virus with SuperFect (Qiagen, Valencia, CA) according to the manufacturer's instructions. Each virus was purified by $CsCl_2$ step gradient ultra-centrifugation followed by $CsCl_2$ linear gradient ultra-centrifugation. The virus particles and biological titer were determined spectrophotometrically by the method of Maizel et al. [29] and by using an Adeno-X Rapid Titer Kit (Clontech, Palo Alto, CA), respectively. The ratio of biological-to-particle titer was 1:22 for Ad-CALacZ, 1:26 for AdRGD-CALacZ, 1:32 for AdK7-CALacZ, and 1:21 for AdF35-CALacZ. The Ad vectors used in the present study were summarized in Table 1.

Cells. Bone marrow-derived hMSCs [purchased from Cambrex Bio Science Walkersville (Walkersville, MD)] were cultured with mesenchymal stem cell basal medium (MSCGM) (Cambrex Bio Science Walkersville) according to the manufacturer's instructions. hMSCs were used for experiments during passages two to four.

Adipocyte differentiation. The adipogenic-differentiated hMSCs were induced according to the manufacturer's instructions (Cambrex Bio Science Walkersville). In brief, hMSCs were seeded at a density of 2.1×10^4 cells/cm^2 and cultured with MSCGM for 10 days. The cells were then cultured with supplemented adipogenesis induction medium (Cambrex Bio Science Walkersville) for 3 days followed by 3 days of culture in supplemented adipogenesis maintenance medium (Cambrex Bio Science Walkersville). After three cycles of induction and maintenance, the cells were cultured with supplemented adipogenesis maintenance medium for 7 days. The differentiation of hMSCs to adipocytes was monitored by measuring intracellular lipid accumulation using Oil red O staining. In brief, the cells were fixed for 2 h with 10% formaldehyde in isotonic phosphate buffer and then washed with distilled water. The cells were then stained with complete immersion in a working solution (0.3%) of Oil red O for 4 h. Excess dye was removed by exhaustive washing with water.

Adenovirus-mediated gene transduction in vitro. hMSCs (1.1×10^4 cells) were seeded into a 24-well dish and the next day the cells were treated with each Ad vector for 1.5 h. Then, the medium containing the vectors was removed and fresh medium (MSCGM) was added to the cells. At the indicated amount of time, LacZ activity in the cells was measured by both X-gal (5-bromo-4-chloro-3-indolyl-β-D-galactopyranoside) staining or the luminescence assay using a luminescent β-galactosidase genetic reporter system II (Clontech).

Flow cytometry. To detect human CAR, the cells (5×10^5 cells) were labeled with mouse monoclonal antibody RmcB (anti-human CAR) (Upstate Biotechnology, Lake Placid, NY) and fluorescein isothiocyanate (FITC)-conjugated goat anti-mouse IgG secondary antibody (Pharmingen, San Diego, CA). To detect human CD46, the cells were labeled with FITC-conjugated anti-human CD46 antibody (Pharmingen). Flow cytometric analysis was performed by a FACSCalibur flow cytometer using CellQuest software (Becton–Dickinson, Tokyo, Japan).

Results and discussion

To develop suitable Ad vectors for hMSCs, various types of fiber-modified Ad vectors expressing LacZ,

Table 1
Adenovirus vectors used in the present study

Name	Fiber type	Promoter
Ad-CALacZ	Type 5 fiber	CA promoter
AdRGD-CALacZ	RGD peptide in the HI loop of the fiber knob	CA promoter
AdK7-CALacZ	Polylysine peptide in the C-terminal of the fiber knob	CA promoter
AdF35-CALacZ	Chimeric type 5 fiber tail and type 35 fiber knob and shaft	CA promoter

CA promoter: β-actin promoter/CMV enhancer with β-actin intron.

which exhibit different tropisms than the conventional Ad vectors, were constructed (Table 1). The CA promoter, which is a hybrid promoter consisting of a β-actin promoter/CMV enhancer with a β-actin intron, was used in the following experiment because this promoter mediates ubiquitous and strong transgene expression [28,30]. Ad-CALacZ contains the wild-type fiber, AdRGD-CALacZ contains an RGD peptide motif in the HI loop of the fiber knob, AdK7-CALacZ contains a polylysine peptide in the C-terminal of the fiber knob, and AdF35-CALacZ contains a fiber protein derived from the Ad type 5 fiber tail and the Ad type 35 fiber knob and shaft. hMSCs were transduced with 100, 300, 1000, or 3000 vector particles (VP)/cell of each vec-

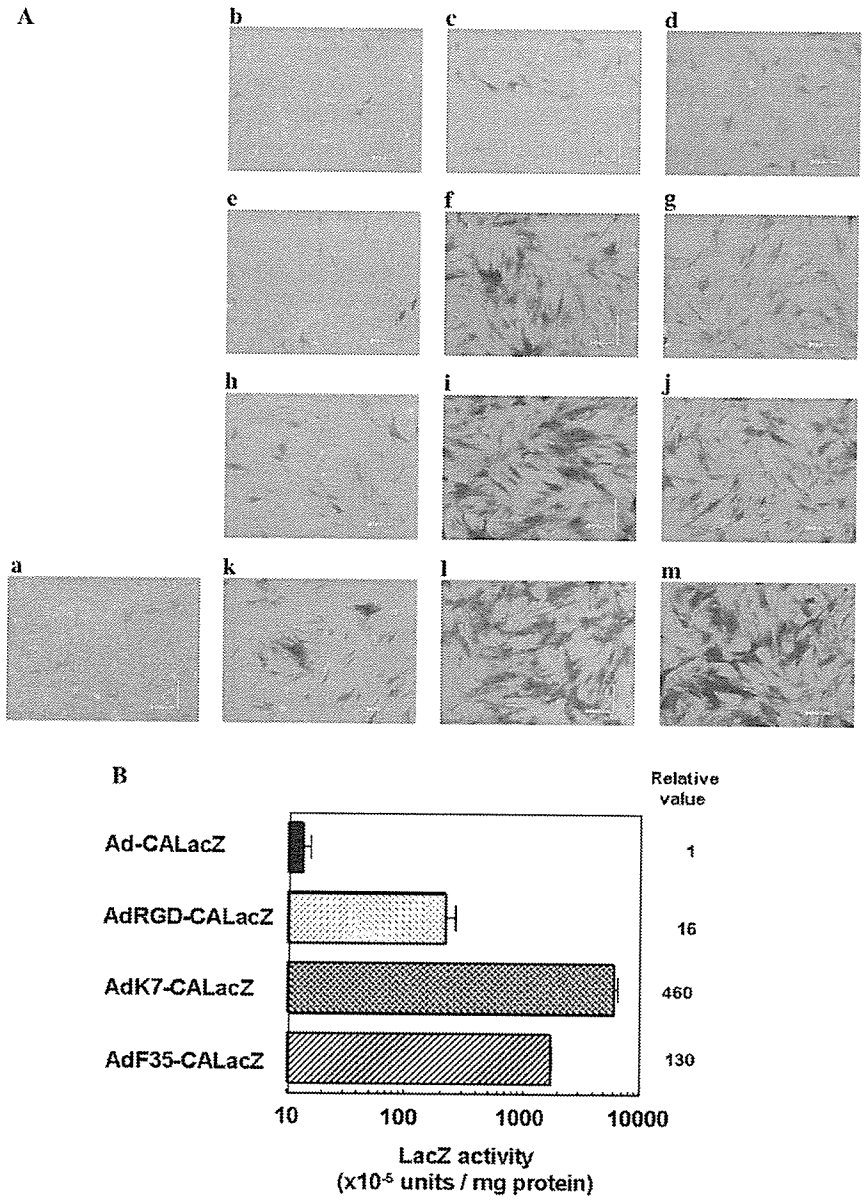

Fig. 1. LacZ expression of hMSCs transduced with various types of fiber-modified Ad vectors. (A) X-gal staining of hMSCs transduced with various types of fiber-modified Ad vectors. hMSCs were transduced with several Ad vectors, each containing one of the following: the wild-type fiber, RGD peptide in the HI loop of the fiber knob, polylysine peptide in the C-terminal of the fiber knob, or Ad type 35 fiber (Ad-CALacZ, AdRGD-CALacZ, AdK7-CALacZ, or AdF35-CALacZ, respectively) at 100, 300, 1000, or 3000 VP/cell for 1.5 h. Then, the medium containing the Ad vectors was removed and fresh medium (MSCGM) was added to the cells. X-gal staining was performed 48 h later. Note that 100% of the hMSCs were X-gal positive by transduction with AdK7-CALacZ (1000 and 3000 VP/cell) and AdF35-CALacZ (3000 VP/cell), and that the cells did not reach confluence. Data of X-gal staining are from one representative experiment of three performed. (a) Ad-CALacZ; (b, e, h, k) AdRGD-CALacZ; (c, f, i, l) AdK7-CALacZ; (d, g, j, m) AdF35-CALacZ. (b, c, d) 100 VP/cell; (e, f, g) 300 VP/cell; (h, i, j) 1000 VP/cell; and (a, k, l, m) 3000 VP/cell. (B) LacZ enzymatic activity of hMSCs transduced with various types of fiber-modified Ad vectors. hMSCs were transduced with 300 VP/cell of Ad-CALacZ, AdRGD-CALacZ, AdK7-CALacZ, or AdF35-CALacZ, respectively, for 1.5 h. Then, the medium containing Ad vectors was removed and fresh medium (MSCGM) was added to the cells. LacZ expression in the cells was measured by a luminescence assay 48 h later. The data of a luminescence assay are expressed as means ± SD ($n = 4$).

tor for 1.5 h, and the LacZ activity was determined by both X-gal staining and the luminescence assay (Fig. 1). In the case of the conventional Ad vector (Ad-CALacZ), the percentage of X-gal-positive cells was low even at the vector concentration of 3000 VP/cell. In contrast, all types of fiber-modified Ad vectors improved transduction efficiency. AdK7-CALacZ was the most effective in transducing the LacZ genes. Direct counting of the percentage of X-gal positive cells suggested that all of the hMSCs were transduced by AdK7-CALacZ at 1000 VP/cell. AdF35-CALacZ also showed high transduction efficiency. AdRGD-CALacZ mediated higher levels of LacZ expression than Ad-CALacZ, but lower levels than AdK7-CALacZ and AdF35-CALacZ (Fig. 1A). A luminescence assay showed that AdK7-CALacZ, AdF35-CALacZ, and AdRGD-CALacZ mediated 460, 130, and 16 times, respectively, the LacZ activity was mediated by Ad-CALacZ (Fig. 1B). Similar results were obtained in hMSCs derived from other donors.

Cytotoxicity and the ability of the transduced hMSCs to differentiate into adipocyte were also examined in hMSCs treated with polylysine-modified Ad vectors. The cell numbers were counted 3 days after transduction. No cytotoxicity was observed in hMSC treated with 1000 VP/cell of AdK7-CALacZ, but a slight cytotoxicity was seen in the cells treated with 3000 VP/cell of AdK7-CALacZ (the cell number was approximately 80% of the non-treated cells) (data not shown). hMSCs transduced with 1000 or 3000 VP/cell of AdK7-CALacZ differentiated into adipocyte as efficiently as non-treated cells (data not shown). Thus, the Ad transduction of hMSCs did not result in any impairment of proliferative and differentiated functions under the condition of 1000 VP/cell.

Tsuda et al. [31] reported that transduction efficiency into rat bone marrow-derived MSCs with an Ad vector containing RGD peptide in the HI loop of the fiber knob was 12 times that of a vector containing the wild-type fiber. Olmsted-Davis et al. [7] reported that human bone marrow-derived MSCs transduced with Ad vectors containing Ad type 35 fiber had higher levels of transgene expression than those transduced with conventional Ad vectors. The results of the present study, which is the first systemic comparison of transduction efficiency using various types of fiber-modified Ad vectors, suggested that polylysine modification of the C-terminal of the fiber knob was the most effective for the transduction of hMSCs.

Next, we examined the time course of transgene expression in hMSCs transduced with the Ad vectors, because the differentiation of hMSCs usually requires long-term cultivation. hMSCs were seeded into a 24-well dish and transduced with 1000 VP/cell of AdK7-CALacZ for 1.5 h. Then, the medium containing the Ad vectors was removed and fresh medium (MSCGM) was added to the cells. The cells reached confluence after 3–4 days and then became contact-inhibited. The cells were cultured without any passages. At days 2, 5, 13, 20, and 33, the LacZ expression in the cells was determined by a luminescence assay (Fig. 2). The results showed that LacZ expression was stable for 33 days, suggesting that Ad vector-mediated gene expression lasts at least a month in the cultured hMSCs when the transduced cells were cultured with contact-inhibition.

To determine why the Ad vector containing the wild-type fiber transduced hMSCs inefficiently, we examined the expression of CAR and CD46 in hMSCs by flow cytometry. The results showed that hMSCs express little CAR but higher levels of CD46 (Fig. 3), reflecting the lower or higher efficiency of gene expression by Ad-CALacZ or AdF35-CALacZ, respectively.

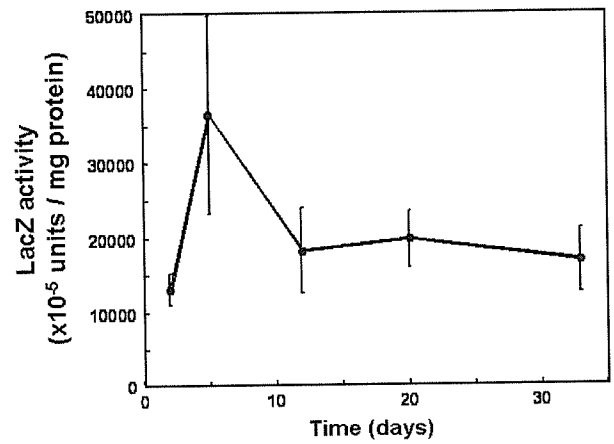

Fig. 2. Time course of LacZ expression in hMSCs transduced with AdK7-CALacZ. hMSCs were transduced with 300 VP/cell of AdK7-CALacZ for 1.5 h. Then, the medium containing Ad vectors was removed and fresh medium (MSCGM) was added to the cells. At the indicated times, LacZ expression in the cells was determined by a luminescence assay. The data of a luminescence assay are expressed as means ± SD ($n = 4$).

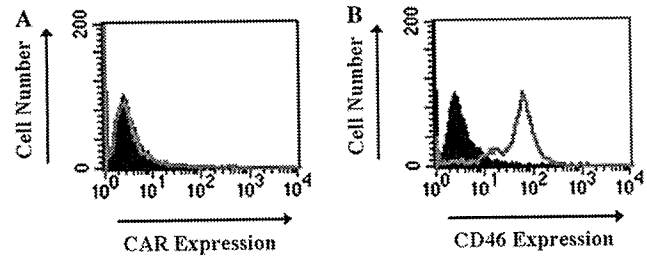

Fig. 3. Flow cytometric analysis of levels of CAR and CD46 expression in hMSCs. hMSCs were labeled with (A) mouse monoclonal antibody RmcB (anti-human CAR) and then FITC-conjugated goat anti-mouse IgG secondary antibody, or (B) FITC-conjugated anti-human CD46 antibody to detect human CAR or CD46 expression, respectively. As a negative control, the cells were incubated with an irrelevant antibody (shaded histogram). Flow cytometric analysis was performed by a FACSCalibur flow cytometer. Data shown are from one representative experiment of three performed.

We further examined the efficiency of transduction of adipogenic-differentiated hMSCs by fiber-modified Ad vectors. The adipocytes were induced from hMSCs according to the manufacturer's instructions (Cambrex Bio Science Walkersville), as described in Materials and methods. The differentiation of hMSCs to adipocytes was monitored by measuring the intracellular lipid accumulation using Oil red O staining (Figs. 4A and B). The transduction experiment was then carried out according to a protocol similar to that used for the hMSCs experiment. The cells were counted just before the experiment. The adipogenic-differentiated hMSCs were infected with each Ad vector at 300 VP/cell, and X-gal staining was performed 2 days later. As shown in Fig. 4C, Ad-CALacZ exhibited negligible LacZ expression in the cells with lipid vacuoles, i.e., the adipogenic-differentiated hMSCs. X-gal-positive cells were obtained in hMSCs without lipid vacuoles (non-adipogenic cells). AdRGD-CALacZ and AdK7-CALacZ led to an increase in LacZ-positive cells, but mediated LacZ expression in non-adipogenic cells (Figs. 4D and E). In sharp contrast, AdF35-CALacZ showed high LacZ expression in adipogenic-differentiated hMSCs only, and not in non-adipogenic cells (Fig. 4F). These results obtained further support from the flow cytometric analysis, in which adipogenic cells expressed high levels of CD46, but low levels of CAR (Fig. 5). The reason why AdF35-CALacZ mediated LacZ expression specifically in the adipogenic-differentiated hMSCs remains unclear, but these results may have been due to differences in the trafficking of the viral genome, relative CA promoter activity, and/or other factors in undifferentiated- vs. adipogenic-differentiated hMSCs. The hMSCs cultured with adipogenic medium expressed slightly more CAR than the uninduced hMSCs (Figs. 3 and 5); thus, the hMSCs cultured with adipogenic medium expressed more LacZ than the hMSCs cultured with normal medium (MSCGM) (Figs. 1 and 4). These results suggested that Ad vectors containing Ad type 35 fiber are of great utility for efficient transduction into adipogenic-differentiated hMSCs, and both RGD and polylysine modification of the fiber knob were found not to be effective for transduction into adipogenic-differentiated hMSCs.

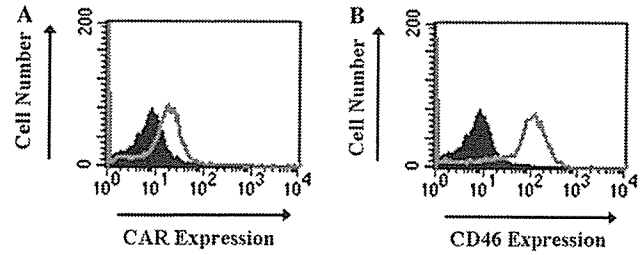

Fig. 5. Flow cytometric analysis of levels of CAR and CD46 expression of adipogenic-differentiated hMSCs. The adipogenic-differentiated hMSCs were labeled with (A) mouse monoclonal antibody RmcB (anti-human CAR) and then FITC-conjugated goat anti-mouse IgG secondary antibody, or (B) FITC-conjugated anti-human CD46 antibody to detect human CAR or CD46 expression, respectively. As a negative control, the cells were incubated with an irrelevant antibody (shaded histogram). Flow cytometric analysis was performed using a FACSCalibur flow cytometer. Data shown are from one representative experiment of three performed.

In summary, polylysine modification of the fiber knob and replacement of Ad type 5 fiber with Ad type 35 fiber in the Ad vectors exhibited the most efficient gene transfer into hMSCs and adipogenic-differentiated hMSCs, respectively. These types of fiber-modified Ad vectors are potentially useful for studies of gene function and also for the therapeutic application of hMSCs.

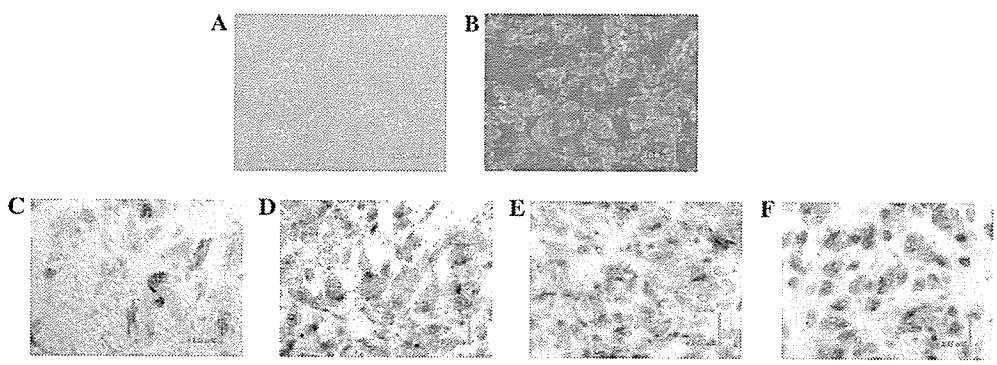

Fig. 4. X-gal staining of adipogenic-differentiated hMSCs transduced with various types of fiber-modified Ad vectors. Adipocytes were induced from hMSCs as described in Materials and methods. Intracellular lipid accumulation, which was used to mark adipocyte differentiation of uninduced (A) and induced hMSCs (B), was determined by Oil red O staining. The adipogenic-differentiated hMSCs were transduced with Ad vectors, each of which contained one of the following: the wild-type fiber (C), RGD peptide in the HI loop of the fiber knob (D), polylysine peptide in the C-terminal of the fiber knob (E), or Ad type 35 fiber (F) (Ad-CALacZ, AdRGD-CALacZ, AdK7-CALacZ, or AdF35-CALacZ, respectively) at 300 VP/cell for 1.5 h. Then, the medium containing Ad vectors was removed and fresh medium (supplemented adipogenesis maintenance medium) was added to the cells. X-gal staining was performed 48 h later. Data shown are from one representative experiment of three performed.

Acknowledgments

We thank Dr. J. Miyazaki for kindly providing the cytomegalovirus enhancer/chicken β-actin promoter/β-actin intron. This work was supported by grants from the Ministry of Health, Labour and Welfare of Japan and by a Grant-in-Aid for Scientific Research on Priority Areas of the Ministry of Education, Culture, Sports, Science and Technology (MEXT) of Japan.

References

[1] D.C. Colter, R. Class, C.M. DiGirolamo, D.J. Prockop, Proc. Natl. Acad. Sci. USA 97 (2000) 3213–3218.
[2] M.F. Pittenger, A.M. Mackay, S.C. Beck, R.K. Jaiswal, R. Douglas, J.D. Mosca, M.A. Moorman, D.W. Simonetti, S. Craig, D.R. Marshak, Science 284 (1999) 143–147.
[3] J. Sanchez-Ramos, S. Song, F. Cardozo-Pelaez, C. Hazzi, T. Stedeford, A. Willing, T.B. Freeman, S. Saporta, W. Janssen, N. Patel, D.R. Cooper, P.R. Sanberg, Exp. Neurol. 164 (2000) 247–256.
[4] D. Woodbury, E.J. Schwarz, D.J. Prockop, I.B. Black, J. Neurosci. Res. 61 (2000) 364–370.
[5] B.E. Petersen, W.C. Bowen, K.D. Patrene, W.M. Mars, A.K. Sullivan, N. Murase, S.S. Boggs, J.S. Greenberger, J.P. Goff, Science 284 (1999) 1168–1170.
[6] P.A. Conget, J.J. Minguell, Exp. Hematol. 28 (2000) 382–390.
[7] E.A. Olmsted-Davis, Z. Gugala, F.H. Gannon, P. Yotnda, R.E. McAlhany, R.W. Lindsey, A.R. Davis, Hum. Gene Ther. 13 (2002) 1337–1347.
[8] M. Studeny, F.C. Marini, R.E. Champlin, C. Zompetta, I.J. Fidler, M. Andreeff, Cancer Res. 62 (2002) 3603–3608.
[9] S.C. Hung, C.Y. Lu, S.K. Shyue, H.C. Liu, L.L. Ho, Stem Cells 22 (2004) 1321–1329.
[10] T.J. Wickham, E. Tzeng, L.L.N. Shears, P.W. Roelvink, Y. Li, G.M. Lee, D.E. Brough, A. Lizonova, I. Kovesdi, J. Virol. 71 (1997) 8221–8229.
[11] I. Dmitriev, V. Krasnykh, C.R. Miller, M. Wang, E. Kashentseva, G. Mikheeva, N. Belousova, D.T. Curiel, J. Virol. 72 (1998) 9706–9713.
[12] V. Krasnykh, I. Dmitriev, G. Mikheeva, C.R. Miller, N. Belousova, D.T. Curiel, J. Virol. 72 (1998) 1844–1852.
[13] H. Mizuguchi, N. Koizumi, T. Hosono, N. Utoguchi, Y. Watanabe, M.A. Kay, T. Hayakawa, Gene Ther. 8 (2001) 730–735.
[14] N. Koizumi, H. Mizuguchi, N. Utoguchi, Y. Watanabe, T. Hayakawa, J. Gene Med. 5 (2003) 267–276.
[15] C. Hidaka, E. Milano, P.L. Leopold, J.M. Bergelson, N.R. Hackett, R.W. Finberg, T.J. Wickham, I. Kovesdi, P. Roelvink, R.G. Crystal, J. Clin. Invest. 103 (1999) 579–587.
[16] J. Gall, A. Kass-Eisler, L. Leinwand, E. Falck-Pedersen, J. Virol. 70 (1996) 2116–2123.
[17] S.C. Stevenson, M. Rollence, J. Marshall-Neff, A. McClelland, J. Virol. 71 (1997) 4782–4790.
[18] M. Chillon, A. Bosch, J. Zabner, L. Law, D. Armentano, M.J. Welsh, B.L. Davidson, J. Virol. 73 (1999) 2537–2540.
[19] D.M. Shayakhmetov, T. Papayannopoulou, G. Stamatoyannopoulos, A. Lieber, J. Virol. 74 (2000) 2567–2583.
[20] H. Mizuguchi, T. Hayakawa, Gene 285 (2002) 69–77.
[21] A. Segerman, J.P. Atkinson, M. Marttila, V. Dennerquist, G. Wadell, N. Arnberg, J. Virol. 77 (2003) 9183–9191.
[22] A. Gaggar, D.M. Shayakhmetov, A. Lieber, Nat. Med. 9 (2003) 1408–1412.
[23] J.J. Short, A.V. Pereboev, Y. Kawakami, C. Vasu, M.J. Holterman, D.T. Curiel, Virology 322 (2004) 349–359.
[24] D. Sirena, B. Lilienfeld, M. Eisenhut, S. Kalin, K. Boucke, R.R. Beerli, L. Vogt, C. Ruedl, M.F. Bachmann, U.F. Greber, S. Hemmi, J. Virol. 78 (2004) 4454–4462.
[25] E. Wu, S.A. Trauger, L. Pache, T.M. Mullen, D.J. von Seggern, G. Siuzdak, G.R. Nemerow, J. Virol. 78 (2004) 3897–3905.
[26] H. Mizuguchi, M.A. Kay, Hum. Gene Ther. 9 (1998) 2577–2583.
[27] H. Mizuguchi, M.A. Kay, Hum. Gene Ther. 10 (1999) 2013–2017.
[28] H. Niwa, K. Yamamura, J. Miyazaki, Gene 108 (1991) 193–199.
[29] J.V.J. Maizel, D.O. White, M.D. Scharff, Virology 36 (1968) 115–125.
[30] Z.-L. Xu, H. Mizuguchi, A. Ishii-Watabe, E. Uchida, T. Mayumi, T. Hayakawa, Gene 272 (2001) 149–156.
[31] H. Tsuda, T. Wada, Y. Ito, H. Uchida, H. Dehari, K. Nakamura, K. Sasaki, M. Kobune, T. Yamashita, H. Hamada, Mol. Ther. 7 (2003) 354–365.

0022-3565/05/3142-789–795$20.00
THE JOURNAL OF PHARMACOLOGY AND EXPERIMENTAL THERAPEUTICS

JPET 314:789–795, 2005

Vol. 314, No. 2
85399/3041353
Printed in U.S.A.

Role of N-Terminal Amino Acids in the Absorption-Enhancing Effects of the C-Terminal Fragment of *Clostridium perfringens* Enterotoxin

Akane Masuyama,[1] Masuo Kondoh,[1] Hirotoshi Seguchi, Azusa Takahashi, Motoki Harada, Makiko Fujii, Hiroyuki Mizuguchi, Yasuhiko Horiguchi, and Yoshiteru Watanabe

Department of Pharmaceutics and Biopharmaceutics, Showa Pharmaceutical University (A.M., M.K., H.S., A.T., M.H., M.F., Y.W.), Machida, Tokyo, Japan; Project III, National Institute of Biomedical Innovation (H.M.), Osaka, Japan; and Department of Bacterial Toxinology, Research Institute for Microbial Diseases, Osaka University (Y.H.), Osaka, Japan

Received February 24, 2005; accepted April 14, 2005

ABSTRACT

We recently found that a polypeptide, the C-terminal of *Clostridium perfringens* enterotoxin (C-CPE), was a novel type of drug absorption enhancer. The C-terminal of C-CPE is thought to play a role in the binding of C-CPE to its receptor, claudin-4; however, the function of the N-terminal of C-CPE is unclear. In the present study, we evaluated the role of the N-terminal domain of C-CPE in jejunal absorption and claudin-4 binding. The treatment of rat jejunum with C-CPE resulted in enhanced absorption of dextran, with a molecular weight of 4000 Da. However, treatment with C-CPE220, which lacks the 36 N-terminal amino acids of C-CPE, did not enhance jejunal absorption. C-CPE had affinity for claudin-4 in rat jejunum lysates and Caco-2 lysates, but C-CPE220 did not. Interaction of C-CPE with the recombinant extracellular domain 2 of human claudin-4 (EC2hCld-4), which is the putative binding site for C-CPE, was observed, but C-CPE220 had no affinity for EC2hCld-4. To investigate the effect of C-CPE220 on the barrier function of tight junctions, we measured transepithelial electric resistance (TER) in C-CPE- or C-CPE220-treated Caco-2 monolayer cells. Although C-CPE decreased TER in Caco-2 monolayer cells, C-CPE220 did not disrupt the barrier function of tight junctions. Together, these results indicate that the 36 N-terminal amino acids of C-CPE may be necessary for the enhanced absorption mediated by C-CPE and play a partial role in binding to claudin-4.

Tight junctions (TJs) are the most apical component of intracellular junctional complexes and play a central role in sealing the intercellular space in epithelial and endothelial cellular sheets (Gumbiner, 1993; Anderson and Van Itallie, 1995; Tsukita and Furuse, 2000). Thus, TJs establish cell polarity and are major determinants of paracellular permeability (Chen et al., 1997). There are three types of integral membrane proteins in TJs: occludin (Furuse et al., 1993), junctional adhesion molecule (Martin-Padura et al., 1998), and claudin (Furuse et al., 1998). Using knockout mice and a modulator of claudin, claudin was found to be an essential component for the maintenance of the barrier function of TJs (Balda et al., 1996; Saitou et al., 1998; Sonoda et al., 1999; Furuse et al., 2002; Nitta et al., 2003). Claudin has a molecular mass of ~23 kDa and contains four transmembrane domains. The claudin family consists of at least 24 members that form homodimers and heterodimers in TJs (Heiskala et al., 2001). The tightness of TJs is speculated to be determined by the combination of claudin family members (Furuse et al., 1999; Tsukita and Furuse, 2000). Many members of the claudin family show a distinct organ-specific distribution pattern (Rahner et al., 2001; Tsukita et al., 2001); the variation of expression profiles of claudin family members may be a critical factor that determines paracellular permeability in a tissue. Claudin-5-deficient mice had a leaky blood-brain barrier that allowed the transfer of a ~800-Da molecular from systemic circulation into brain (Nitta et al., 2003). The epidermal barrier was disrupted in claudin-1-deficient mice

[1] These authors equally contributed to this work.

This study is partly supported by a grant-in-aid from the Ministry of Education, Culture, Sports, Science and Technology (Japan).

Article, publication date, and citation information can be found at http://jpet.aspetjournals.org.

doi:10.1124/jpet.105.085399.

ABBREVIATIONS: TJ, tight junction; CPE, *Clostridium perfringens* enterotoxin; C-CPE, C-terminal fragment of *Clostridium perfringens* enterotoxin; CPE-R, *Clostridium perfringens* enterotoxin receptor; PBS, phosphate-buffered saline; PAGE, polyacrylamide gel electrophoresis; FD-4, fluorescein isothiocyanate-dextran with a molecular mass of 4000 Da; AUC_{0-4}, area under the plasma concentration-time curve from 0 to 4 h; Ab, antibody; GST, glutathione *S*-transferase; EC2hCld-4, extracellular domain 2 of human claudin-4; aa, amino acid; TER, transepithelial electric resistance; AUC, the area under the plasma concentration-time curve; Ni-NTA, nickel-nitrilotriacetic acid.

(Furuse et al., 2002). These results indicate that the modulation of claudin in a family member-specific manner can be a potent method to create a tissue-specific drug delivery system.

Clostridium perfringens enterotoxin (CPE), a single polypeptide with a molecular weight of ~35 kDa, is the causative agent of symptoms associated with *Clostridium perfringens* food poisoning in humans (McClane et al., 1988). CPE produced in the intestinal tract during sporulation injures intestinal epithelial cells and causes fluid accumulation in the intestinal cavity, which results in diarrhea (Stark and Duncan, 1971). This effect of CPE is caused by the binding of COOH terminus fragment (C-CPE) to its receptors, an unknown ~45- to 50-kDa protein and the ~23-kDa protein (CPE-R), which consists of 209 amino acids and contains four putative transmembrane domains (McClane and Chakrabarti, 2004). After C-CPE binds to CPE-R, pores form on the mucosal membrane; these pores cause massive changes in small molecule permeability, osmotic cell ballooning, and cytolysis (McClane, 1984; Wieckowski et al., 1994; Katahira et al., 1997). Recently, the CPE-R was identified as claudin-4, a member of the claudin multigene family (Sonoda et al., 1999). Functional domain mapping of the full-length 319 amino acid CPE protein proved that the CPE290 to CPE319 C-CPE is sufficient for high-affinity binding to the target cell receptor; however, C-CPE is incapable of initiating cytolysis (Kokai-Kun and McClane, 1996, 1997a,b). C-CPE inhibited the barrier function of claudin-4 in MDCK monolayer cells (Sonoda et al., 1999). We found that C-CPE enhanced drug absorption in rat jejunum without any cytotoxic effects. The drug absorption ability was enhanced 400-fold compared with that of a clinically used enhancer (Kondoh et al., 2005). Thus, C-CPE has the potential to be a useful component of drug delivery systems. Functional domain mapping of C-CPE on modulation of claudin-4 is very useful. Although we found that the interaction of C-CPE with claudin-4 via its C-terminal region was responsible for enhanced drug absorption, the detail functional domain of C-CPE to affect TJs is unclear.

In the present study, we evaluated the ability of an NH_2-terminal region of C-CPE to affect TJ barriers and interact with claudin-4. The deletion of 36 amino acids in the N-terminal of C-CPE resulted in decreased affinity for claudin-4 and attenuated TJ modulation. Thus, the 36 amino acids in the N-terminal of C-CPE are necessary for enhanced drug absorption.

Materials and Methods

Animals. Male Wistar rats, weighing 250 to 280 g, were purchased from Japan Laboratory Animals, Inc. (Tokyo, Japan). The rats were cared for according to the guidelines of the ethics committee of Showa Pharmaceutical University, Machida, Tokyo, Japan. The rats were maintained in a room at 23 ± 1.5°C with a 12-h light/dark cycle and were allowed free access to standard rodent chow and water. After their arrival, the rats were given at least 1 week to adapt before the experiments began.

Cell Cultures. Human intestinal epithelial cell line Caco-2 cells are maintained in Dulbecco's modified Eagle's medium containing 10% fetal bovine serum in a 5% CO_2 atmosphere at 37°C. For experiments monitoring the effects of C-CPE on TJ permeability, the cells were seeded Transwell on polycarbonate filter cell culture chamber inserts (6.5-mm diameter, 0.03 cm^2 area, 0.45-μm pore diameter; Costar Europe, Badhoevedorp, The Netherlands). The cells were used for experiments 14 to 21 days after seeding. Passages 60 through 65 were used.

Preparation of 30-Amino Acid Polypeptide. A polypeptide corresponding to 30 amino acids from the C-terminal of C-CPE (NH_2-SLDAGQYVLVMKANSSYSGNYPYSILFQKF-OH) was obtained from Bio-Synthesis (Lewisville, TX). The purity of the peptide was >95%. The peptide was dissolved in phosphate-buffered saline (PBS) buffer and stored at −80°C before use.

Preparation of His-Fused C-CPE220 and C-CPE. To generate histidine-tagged C-CPE220, which lacks the 36 N-terminal amino acids of C-CPE, we used $pETH_{10}PER$ as a template (Katahira et al., 1997). The template was subjected to polymerase chain reaction using the following oligonucleotides: ctcgaggctggtaatttatatgattgg (sense primer for C-CPE220; the underline indicates XhoI site), ctcgagagatgtgttttaacagttcca (sense primer for C-CPE; the underline indicates XhoI site), and ggatcctaaaatttttgaaataatattga (common antisense primer; the underline indicates BamHI site). The resultant fragments of C-CPE220 and C-CPE were subcloned into pGEMTT-Easy vector (Promega, Madison, WI). The sequences of the fragments were confirmed. C-CPE220 was prepared as follows: pGEMTT-Easy vector with C-CPE220 was digested with XhoI/BamHI, and the resultant XhoI-BamHI fragment was inserted into the identical site of pET16b vector. The pET16b plasmid with C-CPE220 was transduced into *Escherichia coli* BL21 (DE3), and the production of C-CPE was stimulated by the addition of isopropyl-β-D-thiogalactopyranoside. The cells were harvested and lysed in buffer A [200 mM phosphate (pH 7.5) and 500 mM NaCl] containing 8 M urea. The lysates were centrifuged, and the resultant supernatant was incubated with Ni-NTA resin (Invitrogen, Carlsbad, CA). C-CPE220 and C-CPE were eluted in a gradient of 0 to 500 mM imidazole in buffer A. The purification of C-CPE220 and C-CPE was confirmed by SDS-PAGE and Western blotting with a His-tagged antibody (Merck, Darmstadt, Germany) (Fig. 3).

In Situ Loop Assay. To evaluate the effects of C-CPEs on the absorption of dextran with a molecular weight of 4000 Da, we performed an in situ closed loop assay. Rats were anesthetized with thiamylal sodium (Mitsubishi Pharma Corporation Ltd, Osaka, Japan). A midline abdominal incision was made, and the lumen of the jejunum was washed with phosphate-buffered saline (pH 6.5). A jejunal loop (5 cm in length) was prepared by closing both ends with sutures. Fluorescein isothiocyanate-dextran with a molecular mass of 4000 Da (FD-4) with or without C-CPEs in 200 μl of PBS was administered into the jejunal loop. Blood was collected from the jugular vein at the indicated periods. The plasma level of FD-4 was measured with a fluorescence spectrophotometer (Fluoroskan Ascent FL; Thermo Electron Corporation, Waltham, MA). The area under the plasma concentration-time curve from 0 to 4 h (AUC_{0-4}) was calculated by the trapezoidal method.

Interaction of Claudin-4 and C-CPEs. To investigate the interactions between claudin-4 and C-CPEs, we used lysates of rat jejunum and Caco-2, in which claudin-4 protein was expressed (Rahner et al., 2001; Singh et al., 2001). Rat mucosa of the corresponding region of the jejunum used in the in situ loop assay was collected with a scraper and washed twice with ice-cold PBS. The mucosa and Caco-2 were lysed in PBS containing 1% protease inhibitor cocktail (Sigma-Aldrich, St. Louis, MO). The concentrations of protein were determined with a commercially available protein assay kit using bovine serum albumin as a protein standard (Pierce, Rockford, IL). After 30 min of incubation of C-CPEs and the lysates at 37°C, nickel beads were incubated with the mixture for an additional 3 h at 4°C. Then, the beads were washed with the lysis buffer, and the complexes that were bound to the beads were solubilized in SDS sample buffer. The complexes were subjected to SDS-PAGE followed by Western blotting for anti-His Ab and anti-claudin-4 Ab (Zymed Laboratories, South San Francisco, CA). Ab-reacted bands were detected using horseradish peroxidase-labeled secondary Ab and enhanced

chemiluminescence reagents (Amersham Biosciences Inc., Piscataway, NJ).

Preparation of Glutathione *S*-Transferase (GST)-Fused EC2hCld-4. To subclone the extracellular domain 2 of human claudin-4 (EC2hCld-4) (141–210 aa), we used a human placenta cDNA library (TaKaRa, Shiga, Japan) as a template. The template was subjected to polymerase chain reaction using gaattccacaacatcatccaagacttctac (the underline indicates EcoRI site) as the sense primer and aagcttacacgtagttgctggcagc (the underline indicates HindIII site) as the antisense primer. The resultant fragments of EC2hCld-4 were subcloned into pGEMTT vector (Promega). The sequences of the fragments were confirmed. The EcoRI-NotI site of pGEMTT-Easy vector with EC2hCld-4 was inserted into the corresponding site of pGEX4T-1 plasmid (Amersham Biosciences Inc.). The GST-fused EC2hCld-4 (GST/EC2hCld-4) was prepared as described previously (Frangioni and Neel, 1993). Briefly, pGEX4T-1 plasmid with EC2hCld-4 was introduced into the *E. coli* BL21 (DE3) strain, and expression of the GST/EC2hCld-4 was induced with isopropyl β-D-thiogalactopyranoside. The *E. coli* cells were harvested and lysed in STE buffer [10 mM Tris-HCl (pH 8.0), 150 mM NaCl, and 1 mM EDTA] containing 100 μg/ml lysozyme, 5 mM dithiothreitol, and 1.5% *N*-lauroylsarcosine. The lysates were centrifuged, and 2% Triton X-100 was added to the supernatant. The supernatant was reacted with glutathione-agarose beads, and the beads were washed with STE buffer. GST/EC2hCld-4 was eluted from the glutathione-agarose beads with STE buffer containing 50 mM glutathione. The solvent of the elutions was exchanged into PBS by dialysis (Amersham Biosciences Inc.). The purification of GST/EChCld-4 was confirmed by SDS-PAGE followed by staining with Coomassie Brilliant Blue and by Western blotting with a GST-tagged antibody (data not shown).

Enzyme-Linked Immunosorbent Assay. Immunoplates (NUNC A/S, Roskilde, Denmark) were coated with 10 μg/ml GST or GST/EC2hCld-4 in 50 mM bicarbonate buffer. After washing the wells with T-TBS (20 mM Tris-HCl pH 7.4, 40 mM NaCl, and 0.05% Tween 20), the wells were blocked with 1% gelatin in TBS (20 mM Tris-HCl, pH 7.4, and 40 mM NaCl) for 2 h at room temperature, and then C-CPEs were added to the wells at the indicated concentrations. After 2 h of incubation at room temperature, the wells were washed once with T-TBS and incubated with anti-His tagged antibody (Novagen) for 2 h at room temperature. Then, the wells were washed with T-TBS followed by 2 h of incubation with horseradish peroxidase-labeled antibody at room temperature. After washing with T-TBS three times and then with distilled water, 3,3′, 5,5′-tetramethylbenzidine was used as a substrate for the labeled antibody. After 10 min of incubation, the color development was terminated by addition of 2 N H_2SO_4. The reaction product was detected by spectrometry at 450 nm. The background reactivity due to nonspecific binding of secondary antibodies was subtracted from the reactivity observed in the presence of primary antibodies.

Measurement of Transepithelial Electric Resistance. To evaluate the effects of C-CPEs on the barrier function of tight junctions in epithelial cells, Caco-2 cells were seeded in Transwell. Transepithelial electric resistance (TER) was measured using a Millicell-ERS epithelial volt-ohmmeter (Millipore Corporation, Billerica, MA) and normalized by the area of the monolayer. The background TER of blank Transwell was subtracted from the TER of cell monolayers.

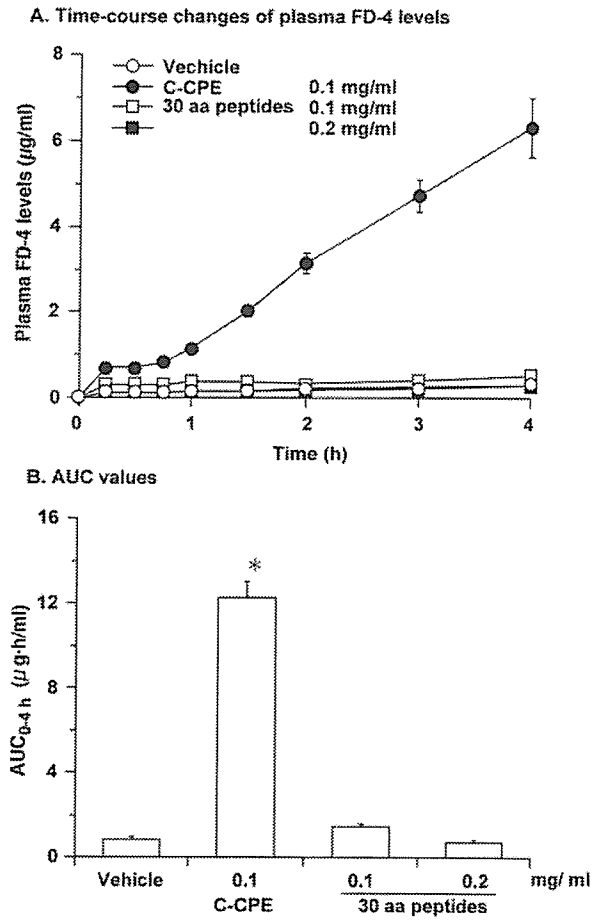

Fig. 2. Effect of receptor-binding domain of CPE on jejunal absorption. Rat jejunum was treated with vehicle or 30-aa peptide. At the indicated point, blood was collected from the jugular vein, and the FD-4 levels in the plasma were measured with a fluorometer (A). The AUC between 0 and 4 h after the treatment was calculated (B). Data are representative of at least three independent experiments. *, significant difference from the vehicle-treated group ($p < 0.05$). Data are means ± S.E. ($n = 4$).

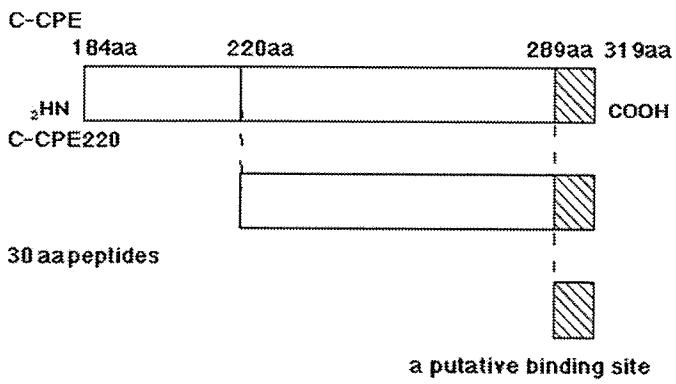

Fig. 1. Schematic representation of C-CPEs and 30-aa peptides used in this study. C-CPE is the C-terminal fragment from amino acid 184 to amino acid 319 of CPE. C-CPE220 does not contain the 36 N-terminal amino acids of C-CPE. The 30-aa peptide consists of only the putative binding region of CPE (Hanna et al., 1991).

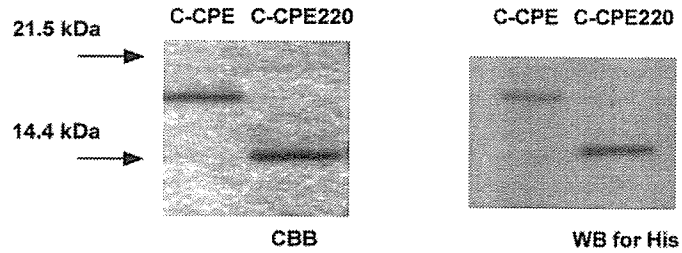

Fig. 3. Purification of C-CPE220. Recombinant C-CPEs were prepared as described in *Materials and Methods*. His-tagged C-CPE and C-CPE220 were subjected to SDS-PAGE, followed by staining with Coomassie Brilliant Blue (CBB), and immunoblot analysis using anti-His-tagged antibody was also performed. WB, Western blot.

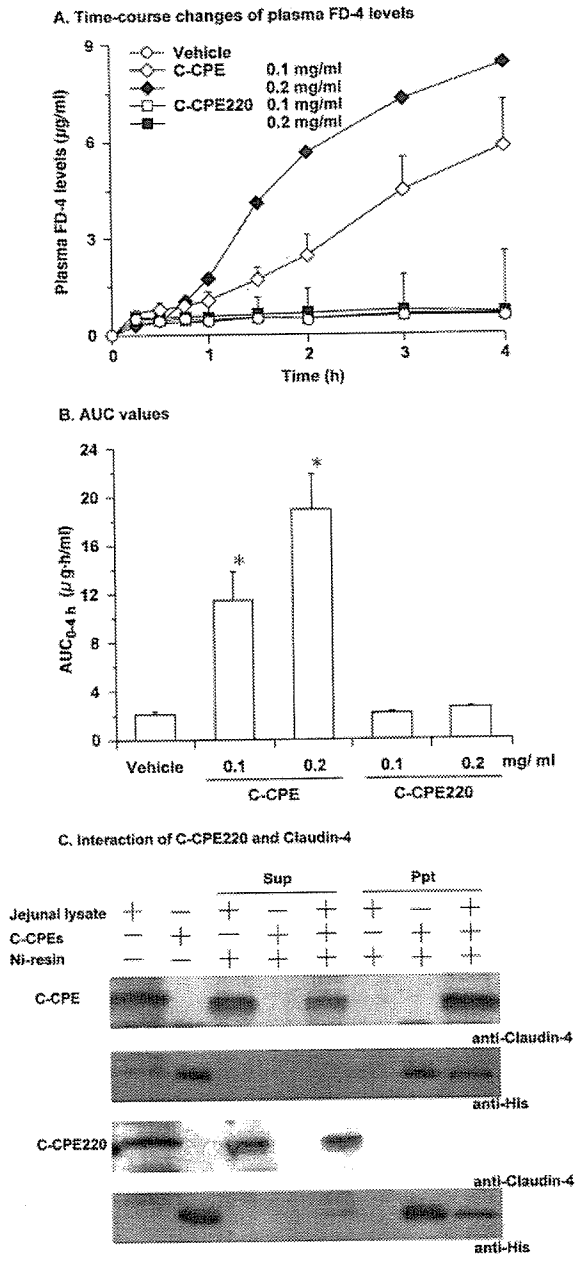

Fig. 4. Effects of C-CPE220 on jejunal absorption in rats. A and B, modulation of rat jejunal absorption of dextran by C-CPE. The effect of C-CPE220 on absorption was assayed by in situ loop assay using rat jejunum. After treatment of rat jejunum with C-CPE or C-CPE220 (0.1 and 0.2 mg/ml), time course changes in plasma FD-4 levels were measured at the indicated periods (A). The AUC value between 0 and 4 h after the treatment was calculated by the trapezoidal method (B). Data are representative of three independent experiments. *, significantly different from the vehicle-treated group ($p < 0.05$). Data are means ± S.E. ($n = 4$). C, interaction of C-CPE220 and claudin-4 in a lysate of rat jejunum. Ten micrograms of C-CPE or C-CPE220 was incubated with the lysate of rat jejunum (200 μg of protein) for 30 min at 37°C. Ni-NTA resin was added, and the mixture was incubated for an additional 3 h at 4°C. Then the samples were centrifuged, and the resultant supernatant fraction (Sup) was prepared. The precipitated resin was washed with the buffer for pull down. The resultant precipitated fraction containing resin (Ppt) was prepared. The Sup and Ppt fractions were subjected to SDS-PAGE followed by immunoblotting using anti-His tagged antibody or anti-claudin-4 antibody. Data are representative of four independent experiments.

Statistical Analysis. Data were analyzed using one-way analysis of variance followed by Dunnett's method. The level of statistical significance was set at $p < 0.05$.

Results

Effects of the N-Terminal Region of C-CPE on the Interaction with Claudin-4. The functional domain of CPE has been investigated (Horiguchi et al., 1986, 1987; Hanna et al., 1991, 1992), and the 30 amino acids at the carboxyl terminal (corresponding to CPE289–319) were speculated to be responsible for the binding of CPE to its receptor (Hanna et al., 1991). C-CPE is the C-terminal fragment of CPE that corresponds to CPE184 to CPE319 (Katahira et al., 1997). We first investigated whether the putative binding region of C-CPE, the 30-aa polypeptide identical to CPE289 to CPE319 (Fig. 1), can modulate jejunal absorption of FD-4. As indicated in Fig. 2, A and B, treatment with C-CPE (0.1 mg/ml) resulted in 12.5-fold increased absorption of FD-4 compared with the vehicle-treated group. However, the 30-aa peptide did not modulate absorption of FD-4 at 0.2 mg/ml. These data indicate that the 30-aa peptide was not enough to modulate absorption. So we next evaluated the involvement of the N-terminal region of C-CPE in the interaction of C-CPE and claudin-4. For this purpose, we prepared recombinant His-tagged C-CPE and C-CPE220, in which the 36 N-terminal amino acids are deleted (Fig. 3). We tried to prepare histidine-fused C-CPE255 and -290, which lacks the 71 N-terminal amino acids and 105 N-terminal amino acids, respectively, but we had no success to prepare them. Therefore, we analyzed effects of C-CPE220 and the synthetic 30-aa polypeptides corresponding to C-CPE290. The molecular weights of the recombinant C-CPEs were confirmed to be the theoretical values (C-CPE, 18 kDa; C-CPE220, 13.8 kDa).

Effects of C-CPE220 on Jejunal Absorption. Since C-CPE has been reported to influence epithelial barrier function in epithelial monolayer cells and enhance the absorption of dextran with a molecular weight of 4000 Da in rat jejunum (Sonoda et al., 1999; Kondoh et al., 2005), we analyzed the effects of C-CPE220 on epithelial barrier function and dextran absorption. To evaluate the effect of C-CPE220 on jejunal absorption in rats, we performed in situ loop assays in rat jejunum, as described previously (Kondoh et al., 2005). Figure 4A shows time course changes in typical plasma FD-4 levels after treatment of the jejunum with C-CPE or C-CPE220. Treatment with C-CPE resulted in absorption of dextran with a molecular weight of 4000 Da. The AUC_{0-4} values in the C-CPE-treated group are 5.3-fold compared with vehicle treatment [AUC_{0-4} = 2.11 ± 0.25 μg · h/ml in vehicle-treated group; AUC_{0-4} = 11.14 ± 2.30 μg · h/ml in C-CPE (0.1 mg/ml)-treated group] (Fig. 4B). However, treatment with C-CPE220 did not elevate the absorption of dextran [AUC_{0-4} = 2.05 ± 0.10 μg · h/ml in C-CPE220 (0.1 mg/ml)-treated group]. These data indicate that the 36 amino acids at the N-terminal of C-CPE might be responsible for enhanced absorption in rat jejunum. To evaluate the interaction between C-CPE220 and claudin-4 in the lysates of rat jejunum, C-CPE or C-CPE220 was incubated with a lysate of rat jejunum, followed by precipitation of the C-CPEs with nickel resin. Interaction between C-CPE220 and claudin-4 was not observed in rat jejunal lysate (Fig. 4C). These data indicate that the 36 amino acids at the N-terminal of C-CPE may play a role in the absorption-enhancing effects of C-CPE.

Effects of C-CPE220 on Tight-Junction Permeability in Caco-2 Monolayer. We investigated whether treatment with C-CPE220 resulted in modulation of tight-junction per-